Available at www.ComputerScienceWeb.com
POWERED BY SCIENCE DIRECT®

Signal Processing 83 (2003) 2227–2258

SIGNAL PROCESSING

www.elsevier.com/locate/sigpro

The frequency spectrum of pulse width modulated signals☆

Zukui Song[1], Dilip V. Sarwate*,[2]

Department of Electrical and Computer Engineering and the Coordinated Science Laboratory, University of Illinois at Urbana-Champaign, Urbana, IL 61801-2397, USA

Received 25 April 2002; received in revised form 13 November 2002

Abstract

The determination of the frequency spectrum of a pulse width modulated (PWM) signal with general band-limited input $x(t)$ has been an open problem for many years. We describe a new approach that gives exact analytical expressions for the spectra of uniform-sampling PWM signals and natural-sampling PWM signals with single-edge as well as with double-edge modulation. For the special case of single tone modulating signals, our results reduce to those obtained previously using a double Fourier series method. We also show that if the maximum magnitude of the derivative of $x(t)$ is smaller than twice the carrier frequency, then a PWM signal consists of a baseband signal $y(t)$ together with $y(t)$ phase-modulated onto each carrier harmonic, where, for uniform-sampling PWM, $y(t)$ is a nonlinear function of the modulating signal $x(t)$, while for natural-sampling PWM, $y(t)$ is just $x(t)$ itself, that is, there is no distortion in the baseband when natural sampling is used.

Keywords: Pulse width modulation; Frequency spectrum; Spectral analysis; Harmonic distortion; Spectral distortion

1. Introduction

Pulse width modulation (PWM) is a well-known technique that has been used for time division multiplexers [3,4], radio frequency transmitters [8], optical data storage [9], control of AC–DC power converters, and the like. More recently, PWM has become important in efficient energy processing and management in all types of communication systems and audio applications [5,10]. The PWM process is a nonlinear modulation, and the demodulation of PWM results in distortion of the modulating signal. In order to understand this distortion, it is important to determine the spectrum of the recovered signal. Unfortunately, this is not easy to do because

☆ This research was supported by a grant from the Motorola Center for Communications at the University of Illinois at Urbana-Champaign.

* Corresponding author.
E-mail addresses: zsong@apogeeddx.com (Z. Song), sarwate@uiuc.edu (D.V. Sarwate).
[1] Present address: Apogee Technology, Inc., 129 Morgan Drive, Norwood MA 02062, USA.
[2] Mailing address: Coordinated Science Laboratory, University of Illinois at Urbana-Champaign, 1308 West Main Street, Urbana, IL 61801-2397, USA.

0165-1684/$ - see front matter © 2003 Elsevier B.V. All rights reserved.
doi:10.1016/S0165-1684(03)00164-6

Nomenclature

Frequency and time variables and constants

f	frequency
f_0	generic constant frequency
f_1	frequency of single-tone sinusoidal signal $x(t)$; one of the frequencies in a two-tone or multitone sinusoidal signal $x(t)$
f_2	frequency of second tone in a two-tone or multitone sinusoidal signal $x(t)$
f_L	cut-off frequency of ideal low-pass filter used as a demodulator for PWM
f_c	carrier or pulse repetition frequency or uniform sampling rate
f_i	frequency of ith tone in multitone sinusoidal signal $x(t)$
f_s	highest frequency in band-limited modulating signal $x(t)$
T	maximum pulse duration or pulse interval; equals f_c^{-1}
t	time
$\hat{t}$	solution to the generalized crossing-point equation for time instant t
$\tilde{t}$	time instant for which t is the solution to the generalized crossing-point equation
$\check{t}$	solution to a modified generalized crossing-point equation for time instant $t + T/2$
$\check{t}$	$\check{t} + T/2$ is the time instant for which t is the solution to the modified generalized crossing-point equation
t_k	location of the trailing edge of the kth pulse in natural-sampling single-edge PWM; solution of the kth crossing-point equation
τ_k	the width of the kth pulse

PWM signals in the time and frequency domains

$P_c(f)$	Fourier transform of square-wave signal $p_c(t)$
$p_c(t)$	a "50% duty cycle" square wave that takes on value $+1$ in intervals $[kT,(k+\frac{1}{2})T)$ and value -1 in intervals $[(k+\frac{1}{2})T,\ (k+1)T)$, $k = \ldots, -2, -1, 0, 1, 2, \ldots$
$P_{DE,A}(f;x)$	Fourier transform of asymmetric double-edge PWM signal $p_{DE,A}(t;x)$
$p_{DE,A}(t;x)$	uniform-sampling asymmetric double-edge PWM signal produced by modulator input $x(t)$
$\hat{p}_{DE,A}(t;x)$	natural-sampling asymmetric double-edge PWM signal produced by modulator input $x(t)$
$P_{DE,S}(t;x)$	Fourier transform of symmetric double-edge PWM signal $p_{DE,S}(t;x)$
$p_{DE,S}(t;x)$	uniform-sampling symmetric double-edge PWM signal produced by modulator input $x(t)$
$\hat{p}_{DE,S}(t;x)$	natural-sampling symmetric double-edge PWM signal produced by modulator input $x(t)$
$p_{LE}(t)$	generic leading-edge PWM signal
$P_{LE}(f;x)$	Fourier transform of leading-edge PWM signal $p_{LE}(t;x)$
$p_{LE}(t;x)$	uniform-sampling leading-edge PWM signal produced by modulator input $x(t)$
$\hat{P}_{LE}(f;x)$	Fourier transform of leading-edge PWM signal $\hat{p}_{LE}(t;x)$
$\hat{p}_{LE}(t;x)$	natural-sampling leading-edge PWM signal produced by modulator input $x(t)$
$P_{s,DE,A}(f;x)$	Fourier transform of $p_{s,DE,A}(t;x)$
$p_{s,DE,A}(t;x)$	the part of the double-edge PWM signal $p_{DE,A}(t;x)$ that depends on $x(t)$
$P_{s,DE,S}(f;x)$	Fourier transform of $p_{s,DE,s}(t;x)$
$p_{s,DE,S}(t;x)$	the part of the double-edge PWM signal $p_{DE,S}(t;x)$ that depends on $x(t)$
$\hat{P}_{s,DE,A}(f;x)$	Fourier transform of $\hat{p}_{s,DE,A}(t;x)$

$\hat{p}_{s,DE,A}(t;x)$ the part of the double-edge PWM signal $p_{DE,A}(t;x)$ that depends on $x(t)$
$\hat{P}_{s,DE,S}(f;x)$ Fourier transform of $\hat{p}_{s,DE,S}(t;x)$
$\hat{p}_{s,DE,S}(t;x)$ the part of the double-edge PWM signal $p_{DE,S}(t;x)$ that depends on $x(t)$
$P_{s,LE}(f;x)$ Fourier transform of $p_{s,LE}(t;x)$
$p_{s,LE}(t;x)$ the part of the leading-edge PWM signal $p_{LE}(t;x)$ that depends on $x(t)$
$P_{s,TE}(f)$ Fourier transform of the generic signal $p_{s,TE}(t)$
$p_{s,TE}(t)$ the part of the trailing-edge PWM signal $p_{TE}(t)$ that depends on the input signal
$P_{s,TE}(f;x)$ Fourier transform of $p_{s,TE}(t;x)$
$p_{s,TE}(t;x)$ the part of the trailing-edge PWM signal $p_{TE}(t;x)$ that depends on $x(t)$
$P_{s,TE}(f;x)$ Fourier transform of $\hat{p}_{s,TE}(t;x)$
$\hat{p}_{s,TE}(t;x)$ the part of the trailing-edge PWM signal $\hat{p}_{TE}(t;x)$ that depends on $x(t)$
$P_{TE}(f)$ Fourier transform of generic trailing-edge PWM signal $p_{TE}(t)$
$p_{TE}(t)$ generic trailing-edge PWM signal
$P_{TE}(f;x)$ Fourier transform of trailing-edge PWM signal $p_{TE}(t;x)$
$p_{TE}(t;x)$ uniform-sampling trailing-edge PWM signal produced by modulator input $x(t)$
$\hat{P}_{TE}(f;x)$ Fourier transform of trailing-edge PWM signal $\hat{p}_{TE}(t;x)$
$\hat{p}_{TE}(t;x)$ natural-sampling trailing-edge PWM signal produced by modulator input $x(t)$

Modulator input and demodulator output signals

$d(t)$ distortion signal that is the difference between the demodulator output and the modulator input signals
$\Phi_x(f)$ energy or power spectral density of $x(t)$
$S_n(f)$ Fourier transform of $(x(t))^n$
$\hat{S}_n(f)$ Fourier transform of $(\hat{x}(t))^n$
$W_n(f)$ Fourier transform of $(1+x(t))^n$
$X(f)$ Fourier transform of $x(t)$
$x(t)$ modulator input signal with maximum amplitude 1; often also assumed to be a low-pass signal with maximum frequency f_s
$\hat{x}(t)$ distorted form of $x(t)$. The natural samples of $x(t)$ are the same as the uniform samples of $\hat{x}(t+T/2)$. Note that $\hat{x}(t)=x(\hat{t})$ and $\hat{x}(\hat{t})=x(t)$
$\check{x}(t)$ another distorted form of $x(t)$. The natural samples of $\check{x}(t)$ are the same as the uniform samples of $x(t+T/2)$. Note that $\check{x}(t)=x(\check{t})$ and $\check{x}(\check{t})=x(t)$
$y(t)$ generic distorted baseband signal in uniform-sampling trailing-edge PWM
$Y(f;x)$ Fourier transform of $y(t;x)$
$y(t;x)$ distorted form of modulator input $x(t)$ produced by the uniform-sampling trailing-edge PWM process in the baseband of the PWM output signal
$Y_k(f;x)$ Fourier transform of $y_k(t;x)$
$y_k(t;x)$ sidebands of the kth carrier harmonic frequency created by the uniform-sampling trailing-edge PWM process with modulator input $x(t)$. Under mild restrictive conditions, $y_k(t;x)$ is equivalent to perfect phase modulation (with phase deviation $\pm k\pi$) of the kth carrier harmonic by $y(t;x)$
$\hat{Y}(f;x)$ Fourier transform of $\hat{y}(t;x)$
$\hat{y}(t;x)$ baseband signal produced by the natural-sampling trailing-edge PWM process with modulator input $x(t)$. Note that $\hat{y}(t;x)=y(t;\hat{x}(t+T/2))$ is also the distorted form of baseband signal produced by uniform sampling of $\hat{x}(t+T/2)$, i.e., $\hat{y}(t;x)=x(t)$

$\hat{y}_k(t;x)$	sidebands of the kth carrier harmonic frequency created by the natural-sampling trailing-edge PWM process with modulator input $x(t)$. Under mild restrictive conditions, $\hat{y}_k(t;x)$ is equivalent to perfect phase modulation (with phase deviation $\pm k\pi$) of the kth carrier harmonic by $\hat{y}(t;x)=x(t)$
$\hat{Y}_k(f;x)$	Fourier transform of $\hat{y}_k(t;x)$
$\tilde{y}(t;x)$	distorted form of modulator input $x(t)$ produced by the uniform-sampling leading-edge PWM process in the baseband of the PWM output signal. Note that $\tilde{y}(t;x)=-y(t;-x)$
$y_{\mathrm{DE,A}}(t;x)$	distorted form of modulator input $x(t)$ produced by the uniform-sampling asymmetric double-edge PWM process in the baseband of the PWM output signal
$y_{\mathrm{DE,S}}(t;x)$	distorted form of modulator input $x(t)$ produced by the uniform-sampling symmetric double-edge PWM process in the baseband of the PWM output signal
$Z(f;x)$	Fourier transform of $z(t;x)$
$z(t;x)$	output of an ideal low-pass filter demodulator for a uniform-sampling trailing-edge PWM signal with modulator input $x(t)$
$\hat{Z}(f;x)$	Fourier transform of $\hat{z}(t;x)$
$\hat{z}(t;x)$	output of an ideal low-pass filter demodulator for a natural-sampling trailing-edge PWM signal with modulator input $x(t)$
$Z_{\mathrm{DE,A}}(f;x)$	Fourier transform of $z_{\mathrm{DE,A}}(t;x)$
$z_{\mathrm{DE,A}}(t;x)$	output of an ideal low-pass filter demodulator for a uniform-sampling asymmetric double-edge PWM signal with modulator input $x(t)$
$Z_{\mathrm{DE,S}}(f;x)$	Fourier transform of $z_{\mathrm{DE,S}}(t;x)$
$z_{\mathrm{DE,S}}(t;x)$	output of an ideal low-pass filter demodulator for a uniform-sampling symmetric double-edge PWM signal with modulator input $x(t)$

Miscellaneous Functions, Variables, and Constants

$a(f)$	generic frequency function
α	complex number
β	complex number
C	contour in the complex plane
$\delta(t)$	impulse function, that is, the Dirac delta function
γ	complex number
i	integer index; integer exponent
$J_n(\cdot)$	Bessel function of the first kind and of integer order n
j	$\sqrt{-1}$
k	integer index
λ	complex number, interior point of contour C
M	amplitude of single-tone sinusoidal signal $x(t)$
M_i	amplitude of ith tone in multitone sinusoidal signal $x(t)$
m	smallest integer such that $mf_{\mathrm{s}}+f_{\mathrm{L}}\geqslant f_{\mathrm{c}}$; also number of tones in multitone sinusoidal signal
$N(n)$	Largest value of k for which the sidebands created by modulation of the kth carrier harmonic by $(x(t))^n$ alias into the low-pass filter pass band
n	integer index; integer exponent
$O(\cdot)$	Bachmann's O-notation as used in asymptotic analysis
$\phi(z)$	analytic function of complex variable z
$\psi(z)$	analytic function of complex variable z

q	inverse of the oversampling ratio
$\mathrm{Re}\{\cdot\}$	the real part of the complex-valued argument
$\mathrm{sgn}(\cdot)$	Signum function with value ± 1 according as the argument is positive or negative
$\mathrm{sinc}(t)$	Sinc function defined as $\sin(\pi t)/\pi t$ for $t \neq 0$ and 1 for $t = 0$
θ	complex variable
$u(t)$	Heaviside step function with value 1 for $t \geqslant 0$ and 0 otherwise
z	complex variable

of the nonlinearities involved. Previous studies [3,10], have used a double Fourier series method to obtain the spectrum of the PWM signal when the modulating signal is a pure sinusoid, that is, a single tone. Extension of this to two-tone signals is messy [3,14], and finding the spectrum of multitone signals analytically is even more complicated. To the best of our knowledge, there is no known general result for the spectrum of the PWM signal when the modulating signal is an arbitrary band-limited signal with finite energy or finite power.

We wish to make it clear that by "spectrum" we mean the Fourier transform of the deterministic PWM signal that results from the application of a deterministic signal to the input of a pulse width modulator. Since the PWM signal is a finite-power signal, this transform exists in the generalized sense. Our interest is in determining how accurately the input signal can be recovered via a demodulator consisting of a lowpass filter (and what is the residual distortion in the demodulated signal) with a view to using PWM in a high-efficiency high-fidelity audio amplifier [13]. The word spectrum can also mean the power density spectrum of the random PWM signal that results when the modulator input is a random process instead of a deterministic signal. Some results on these power density spectra can be found in Middleton's classic text [11]. More recently, the power density spectra of random PWM signals have been the subject of much study (see for example [2,7,16,17,19]) because such random signals can be used for reduction of acoustic noise and resonant vibrations in inverter-based motor drives and for ripple control and spectral shaping in power converters. Indeed, the pulse widths can be dithered in random fashion to achieve the desired effect. However, these applications are not of interest here: we are interested only in deterministic input signals, and in recovering the input waveform as accurately as possible.

In a *single-edge* PWM signal, the position of either the *trailing edge* or the *leading edge* of each pulse is determined by the input (modulating) signal while the other edge occurs at a fixed time. The corresponding signals are called trailing-edge PWM (TEPWM) and leading-edge PWM (LEPWM) signals, respectively. We study the time- and frequency-domain representations of TEPWM and LEPWM signals in Section 2 under the assumption that the modulating signal is a continuous finite energy or finite power signal $x(t)$. We use elementary Fourier analysis to obtain the spectrum of the TEPWM signal produced by *uniform sampling* of $x(t)$ (at rate f_c samples per second) in terms of the spectra of $(x(t))^n$, $n \geqslant 1$. Next, we use an inversion theorem due to Lagrange to extend this result to the spectrum of the TEPWM signal obtained by *natural sampling* of $x(t)$, subject only to the mild condition that the magnitude of the derivative of $x(t)$ is smaller than $2f_c$, that is, twice the sampling rate (or carrier frequency) f_c. Now, $x(t)$ is usually chosen to be a low-pass signal of bandwidth $f_s \ll f_c$ because this allows the use of a low-pass filter as a demodulator for PWM. For such low-pass signals, we show that the derivative of $x(t)$ satisfies the bound if f_c is larger than πf_s. For the special cases of $x(t)$ being a single-tone signal or two-tone signal, our results reduce to those obtained previously [21]. We also show that subject to the magnitude of the derivative of $x(t)$ being bounded by $2f_c$, a TEPWM signal consists of a baseband signal $y(t)$ together with $y(t)$ *phase-modulated* onto each harmonic of the carrier frequency. For uniform-sampling TEPWM, $y(t)$ is a distorted form of the modulating signal $x(t)$ while for natural-sampling TEPWM, $y(t)$ is just $x(t)$ itself. This result proves in more generality a property of natural-sampling PWM that has been noted previously only for sinusoidal signals, namely, there is no signal harmonic distortion in the baseband. In particular, when $x(t)$ is a low-pass signal with bandwidth

f_s, our results show explicitly that low-pass filtering of the natural-sampling PWM signal suffices to recover $x(t)$ perfectly, and that the residual distortion caused by aliasing can be reduced significantly by using a carrier frequency $f_c \gg \pi f_s$. Low-pass filtering of uniform-sampling PWM recovers a distorted form of the modulating signal $x(t)$ and our results exhibit this distortion explicitly for arbitrary modulating signals. Previously, most of these results had been proved analytically only for sinusoidal signals. Because of the close relationship between TEPWM and LEPWM signals, all the above properties are also enjoyed by LEPWM signals with minor differences in various formulas, the details of which are also given in Section 2.

In a *double-edge* PWM signal, the positions of *both* edges of each pulse are determined by the modulating signal. In *symmetric* double-edge PWM, the locations of the midpoints of the pulses are spaced at uniform intervals of T and for each pulse, the location of both the leading edge and trailing edge are determined by one sample of the modulating signal. In *asymmetric* double-edge PWM, the locations of the leading edge and the trailing edge are determined by two different samples of the modulating signal, thus effectively doubling the sampling rate. In Section 3, we show that a double-edge PWM signal can be decomposed into the sum of a TEPWM signal and a LEPWM signal. This allows us to use our results of Section 2 to deduce the spectra of double-edge PWM signals very easily. In particular, we show that there are no carrier harmonics in a natural-sampling asymmetric double-edge PWM signal—all the power is in terms that depend on the modulating signal. In Section 4, we apply our new analytical techniques to sinusoidal modulating signals and show that we get the same results as given by the previous double Fourier series approaches, and that our analysis provides these results, as well as other more general results, very easily. Concluding remarks are in Section 5 of the paper.

2. Single-edge PWM signals with general modulation

2.1. The single-edge modulation process

A single-edge PWM signal consists of a sequence of rectangular pulses that start (or end) at fixed times and whose width depends on the value of samples of the modulating signal. When these samples are uniformly spaced in time, the resulting PWM signal is called a uniform-sampling PWM signal. Natural-sampling PWM is more complicated than uniform-sampling PWM, but it has certain advantages over uniform-sampling PWM, as we shall describe in more detail later in this section. PWM signals resulting from both these sampling methods are shown in Fig. 1.

Assume without loss of generality that the modulating signal $x(t)$ is a bounded continuous function such that $|x(t)| \leqslant 1$ for all t. A pulse-width modulator compares $x(t)$ (or $-x(t)$) to a sawtooth *carrier signal* of period T (the *sampling period* or interval) and fundamental frequency $f_c = T^{-1}$ (the *carrier frequency*) as illustrated in the first graph in Fig. 1. The kth pulse interval is $[kT,(k+1)T)$ during which the carrier ramp sweeps from value -1 at $t = kT$ to value $+1$ at $t = (k+1)T$. Thus, during the kth pulse interval, the carrier ramp can be expressed as $2t/T - (2k+1)$.

Uniform-sampling PWM: In uniform-sampling *trailing-edge* PWM, the leading edge of the kth pulse occurs at time $t = kT$ while the trailing edge occurs at $t = kT + T[1 + x(kT)]/2$, the time instant at which $x(kT)$, the kth *uniform* sample value, equals the carrier ramp $2t/T - (2k+1)$. A uniform-sampling TEPWM signal $p_{TE}(t;x)$ is illustrated in the second graph in Fig. 1. Note that the kth pulse width τ_k is $\tau_k = T[1 + x(kT)]/2$. In contrast, in the uniform-sampling *leading-edge* PWM signal $p_{LE}(t;x)$ illustrated in the third graph in Fig. 1, the trailing edge of the kth pulse is at time $t = (k+1)T$ while the leading edge occurs at $t = kT + (T - \tau_k)$, the time instant at which $-x(kT)$ equals the carrier ramp $2t/T - (2k+1)$. Note that in uniform-sampling PWM, the kth pulse width is the same regardless of whether trailing-edge or leading-edge modulation is being used.

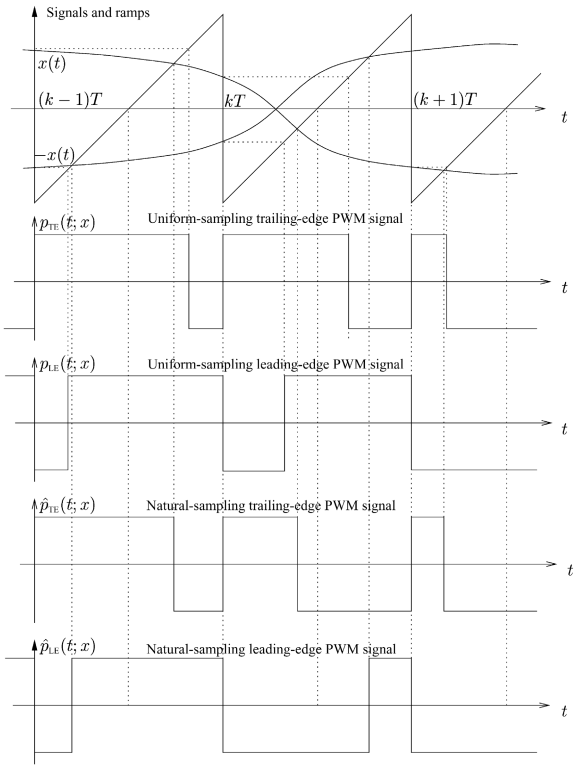

Fig. 1. Single-edge pulse width modulation.

Natural-sampling PWM: In natural-sampling *trailing-edge* PWM, the leading edge of the kth pulse occurs at time $t=kT$ but the trailing edge occurs at the time instant t_k at which $x(t)$ equals the carrier ramp, that is, the location of the trailing edge is given implicitly by the equation $t_k=kT+T[1+x(t_k)]/2$. A natural-sampling TEPWM signal $\hat{p}_{\mathrm{TE}}(t;x)$ is illustrated in the fourth graph in Fig. 1. Similarly, in natural-sampling LEPWM, the trailing edge of the kth pulse is at time $t=(k+1)T$ while the location of the leading edge is given implicitly by the equation $t_k=kT+T[1-x(t_k)]/2$. The natural-sampling LEPWM signal $\hat{p}_{\mathrm{LE}}(t;x)$ is illustrated in the fifth graph in Fig. 1. Note that in contrast to uniform-sampling PWM, the kth pulse width in natural-sampling PWM generally depends on whether trailing-edge or leading-edge modulation is being used.

Natural-sampling PWM requires the comparison of $x(t)$ with a ramp signal whereas uniform-sampling only requires sampling of $x(t)$ at uniformly-spaced intervals. Both methods can be implemented fairly easily for any given analog modulating signal. However, in many cases, the analog signal $x(t)$ is not available explicitly, but is known only through its (uniformly spaced) sample values. In such cases, uniform-sampling PWM is much easier to implement than natural-sampling PWM since the latter requires that either $x(t)$ be reconstructed via interpolation filtering and then compared to the carrier ramp, or the natural sampling pulse widths be computed somehow from the uniform samples of $x(t)$. Although natural-sampling PWM is more difficult to implement in such cases, it is still worth implementing because of its superior distortion performance.

Trailing-edge versus leading-edge PWM: Suppose that the input to a trailing-edge pulse-width modulator is changed from $x(t)$ to $-x(t)$. From the description of the modulation process and Fig. 1, it is easy to see that the resulting TEPWM signal is the *negative* (or complement) of the LEPWM signal that would be

produced by a leading-edge pulse-width modulator with input $x(t)$. Hence, the properties of LEPWM signals are readily deduced from those of TEPWM signals. For this reason, we study only TEPWM signals in detail in this paper, and briefly indicate the minor modifications that must be made in order to apply our results to LEPWM signals.

2.2. The signal-dependent TEPWM signal

Regardless of the type of sampling being used, a trailing-edge pulse-width modulator with input identically 0 produces as its output the 50% duty-cycle square wave $p_c(t)$ that takes on value $+1$ for $kT \leqslant t < (k+\frac{1}{2})T$ and value -1 for $(k+\frac{1}{2})T \leqslant t < (k+1)T$. For nonzero inputs, a *generic* TEPWM signal can be expressed as

$$p_{TE}(t) = p_c(t) + 2\sum_{k=-\infty}^{\infty} u(t-(k+\tfrac{1}{2})T) - u(t-kT-\tau_k), \tag{1}$$

where the kth pulse width τ_k depends on the input signal and the type of sampling. The sum in (1) is the *signal-dependent* part $p_{s,TE}(t)$ of the generic TEPWM signal, and consists of a sequence of positive or negative pulses of duration $|\tau_k - T/2|$. If $\tau_k > T/2$, the kth pulse is positive, and begins at $t=(k+\frac{1}{2})T$ while if $\tau_k < T/2$, the kth pulse is negative, and ends at $t=(k+\frac{1}{2})T$. Thus, $p_{s,TE}(t)$ can be thought of as a composite pulse train in which *trailing-edge* PWM (with positive pulses) is being used when $\tau_k > T/2$, and *leading-edge* PWM (with negative pulses) is being used when $\tau_k < T/2$. Regardless of the value of τ_k, however, the fixed pulse edges in $p_{s,TE}(t)$ always occur at $t=(k+\frac{1}{2})T$.

The TEPWM signal $p_{TE}(t) = p_c(t) + p_{s,TE}(t)$ in (1) is a finite power signal and thus its Fourier transform $P_{TE}(f)$ exists in the generalized sense. Let $P_c(f)$ and $P_{s,TE}(f)$ denote the Fourier transforms of $p_c(t)$ and $p_{s,TE}(t)$, respectively. Since it is well-known that

$$p_c(t) = \sum_{k=0}^{\infty} \frac{4}{(2k+1)\pi}\sin(2\pi(2k+1)f_c t) \tag{2}$$

and

$$P_c(f) = \sum_{k=0}^{\infty} \frac{2}{j(2k+1)\pi}[\delta(f-(2k+1)f_c) - \delta(f+(2k+1)f_c)], \tag{3}$$

we only need to determine the signal-dependent spectrum $P_{s,TE}(f)$ in order to obtain $P_{TE}(f)=P_c(f)+P_{s,TE}(f)$. Now, the pulse $2[u(t-(k+\frac{1}{2})T) - u(t-kT-\tau_k)]$ has Fourier transform $(j\pi f)^{-1}[\exp(-j2\pi f(k+\frac{1}{2})T) - \exp(-j2\pi f(kT+\tau_k))]$, and hence

$$P_{s,TE}(f) = \frac{1}{j\pi f}\sum_{k=-\infty}^{\infty} \exp(-j2\pi f(k+\tfrac{1}{2})T) - \exp(-j2\pi f(kT+\tau_k)). \tag{4}$$

Since τ_k has different values in uniform-sampling PWM and natural-sampling PWM, it is necessary to consider the two cases separately.

2.3. The spectra of uniform-sampling TEPWM signals

In a uniform-sampling TEPWM scheme, the kth pulse width τ_k equals $T[1+x(kT)]/2$. We use $p_{s,TE}(t;x)$ to denote the signal-dependent part of the TEPWM signal, and $P_{s,TE}(f;x)$ to denote its Fourier transform.

From (4) we get that

$$P_{s,TE}(f;x) = \frac{\exp(-j\pi fT)}{j\pi f} \sum_{k=-\infty}^{\infty} \exp(-j2\pi fkT)[1 - \exp(-j\pi fTx(kT))]$$

$$= \frac{\exp(-j\pi fT)}{j\pi f} \sum_{k=-\infty}^{\infty} \exp(-j2\pi fkT) \sum_{n=1}^{\infty} - \frac{(-j\pi fTx(kT))^n}{n!} \tag{5}$$

$$= \frac{\exp(-j\pi fT)}{j\pi f} \sum_{n=1}^{\infty} - \frac{(-j\pi fT)^n}{n!} \sum_{k=-\infty}^{\infty} (x(kT))^n \exp(-j2\pi fkT)$$

$$= \exp(-j\pi fT) \sum_{k=-\infty}^{\infty} \sum_{n=1}^{\infty} \frac{(-j\pi fT)^{n-1}}{n!} S_n(f - kf_c), \tag{6}$$

where $S_n(f)$ is the Fourier transform of $(x(t))^n$ and we have used the discrete-time Fourier transform (DTFT) formula [12] in the last step. The overall spectrum $P_{TE}(f;x)$ of a uniform-sampling TEPWM signal is thus $P_c(f)+P_{s,TE}(f;x)$ where $P_c(f)$ is given in (3) and $P_{s,TE}(f;x)$ is given in (6). Note that $P_c(f)$, the spectrum of the square wave, consists of the carrier signal of frequency f_c and all its *odd*-order harmonics with amplitudes decreasing inversely with order. The *even*-order carrier harmonics including the zeroth order harmonic (or "DC term") are not present in $P_c(f)$. However, as we shall see below, $P_{TE}(f;x) = P_c(f) + P_{s,TE}(f;x)$ contains *all* the carrier harmonics with amplitudes decreasing inversely with order. We consider $P_{s,TE}(f;x)$ and $p_{s,TE}(t;x)$ in more detail. Let

$$P_{s,TE}(f;x) = Y(f;x) + \sum_{k=1}^{\infty} Y_k(f;x),$$

where

$$Y(f;x) = \exp(-j\pi fT) \sum_{n=1}^{\infty} \frac{(-j\pi fT)^{n-1}}{n!} S_n(f)$$

$$= \exp(-j\pi fT) \left[X(f) + \sum_{n=2}^{\infty} \frac{(-j\pi fT)^{n-1}}{n!} S_n(f) \right], \tag{7}$$

and

$$Y_k(f;x) = \exp(-j\pi fT) \sum_{n=1}^{\infty} \frac{(-j\pi fT)^{n-1}}{n!} [S_n(f - kf_c) + S_n(f + kf_c)]. \tag{8}$$

Thus $p_{s,TE}(t;x)$ includes a signal $y(t;x)$ with spectrum $Y(f;x)$ given by (7). It is easy to see that

$$y(t;x) = x(t - T/2) + \sum_{n=2}^{\infty} \frac{1}{n!} \left(\frac{-T}{2} \right)^{n-1} \frac{d^{n-1}}{dt^{n-1}} [x(t - T/2)]^n. \tag{9}$$

Eq. (9) shows that the uniform-sampling TEPWM signal contains the modulating signal $x(t)$ delayed by $T/2$ as well as considerable nonlinear distortion (the terms in the summation on n in (9)) arising from the derivatives of the powers of $x(t - T/2)$. Fortunately, the distortion terms are reduced in amplitude as n increases. In addition to derivatives of the powers of $x(t - T/2)$, the uniform-sampling TEPWM signal also includes signal

terms $y_k(t;x)$, $k>0$, whose spectra $Y_k(f;x)$ are given by (8). Note that

$$y_k(t;x) = 2\sum_{n=1}^{\infty}\frac{1}{n!}\left(\frac{-T}{2}\right)^{n-1}\frac{\mathrm{d}^{n-1}}{\mathrm{d}t^{n-1}}[[x(t-T/2)]^n\cos(2\pi k f_c(t-T/2))]$$

$$= 2(-1)^k\sum_{n=1}^{\infty}\frac{1}{n!}\left(\frac{-T}{2}\right)^{n-1}\frac{\mathrm{d}^{n-1}}{\mathrm{d}t^{n-1}}[[x(t-T/2)]^n\cos(2\pi k f_c t)] \tag{10}$$

is a signal at frequency kf_c.

We remark that the above results are perfectly general and require only that $|x(t)|\leqslant 1$. However, in PWM applications, it is usually assumed that $x(t)$ is strictly band limited to the *signal bandwidth* f_s, that is, its Fourier transform $X(f)$ satisfies

$$X(f)=0 \text{ if } |f|>f_s$$

and that $f_c\geqslant 2f_s$. The latter condition is required in order to recover $x(t)$ from the PWM signal without aliasing effects. Note that this is the same criterion as with pulse-amplitude modulated (PAM) signals, but with PWM signals, requiring that $f_c\geqslant 2f_s$ does not guarantee perfect reconstruction—some residual nonlinear distortion is always present. We shall see that the distortion performance improves as the *oversampling ratio* f_c/f_s increases. In Section 2.8, we show that if the magnitude of the derivative of $x(t)$ is smaller than $2f_c$ (which holds whenever $x(t)$ is band limited to f_s where $\pi f_s<f_c$), then the signal $y_k(t;x)$ in (10) can be expressed as

$$y_k(t;x)=\frac{2(-1)^k}{k\pi}[\sin(2\pi k f_c t)-\sin(2\pi k f_c t-k\pi y(t;x))], \tag{11}$$

which can be recognized as the difference of the kth carrier harmonic and the *phase modulation* of the kth carrier harmonic by $y(t;x)$. From (11) and (2) we can write the TEPWM signal $p_{\mathrm{TE}}(t;x)$ obtained by uniform sampling of $x(t)$ as

$$p_{\mathrm{TE}}(t;x)=y(t;x)+\sum_{k=1}^{\infty}\frac{2}{k\pi}[\sin(2\pi k f_c t)-(-1)^k\sin(2\pi k f_c t-k\pi y(t;x))], \tag{12}$$

where $y(t;x)$ is given by (9). Note that $p_{\mathrm{TE}}(t;x)$ contains every carrier harmonic with amplitude decreasing inversely with order, and also the signal $y(t;x)$ in the baseband together with $y(t;x)$ phase-modulated onto every carrier harmonic.

Finally, we give a heuristic explanation of the fact that the input signal $x(t)$ appears with a delay of $T/2$ in the output of the uniform-sampling TEPWM demodulator. Consider first that $x(t)$ can be recovered perfectly by ideal lowpass filtering of an impulse train in which the kth impulse has amplitude $T\cdot x(kT)$. If the impulse train is delayed by $T/2$ so that the kth impulse occurs at $t=(k+\frac{1}{2})T$ instead of at $t=kT$, then the filter output is also delayed by $T/2$ and is thus $x(t-T/2)$. But, in uniform-sampling TEPWM, the signal $p_{\mathrm{s,TE}}(t;x)$ does not have any impulses. Instead, $p_{\mathrm{s,TE}}(t;x)$ consists of pulses of amplitude $2\cdot\mathrm{sgn}(x(kT))$ and duration $|T\cdot x(kT)/2|$ that have total "area" $2\cdot\mathrm{sgn}(x(kT))\cdot|T\cdot x(kT)/2|=T\cdot x(kT)$. This is the same as the "area" of the impulse $T\cdot x(kT)\delta(t-(k+\frac{1}{2}))T$. Furthermore, the pulses comprising $p_{\mathrm{s,TE}}(t;x)$ either begin or end at $t=(k+\frac{1}{2})T$. Thus, when $p_{\mathrm{s,TE}}(t;x)$ is the input to an ideal lowpass filter, then *to a first approximation,* the output of the filter should be $x(t-T/2)$. But, of course, distortion is present when PWM is used since the impulses have been replaced by fixed-amplitude pulses that do not occur at exactly the same time as the impulses. We show below that the amount of this distortion is roughly the term $(T/2)x(t-T/2)(\mathrm{d}/\mathrm{d}t)x(t-T/2)$ on the right-hand side of (17).

2.4. Demodulation of uniform-sampling TEPWM signals

When $x(t)$ is a low-pass signal of bandwidth f_s, much of the distortion represented by the signals $y_k(t;x)$ can be eliminated by low-pass filtering. That is, a simple demodulator for a PWM signal consists of an ideal low-pass filter with cut-off frequency f_L, where $f_s \leqslant f_L$. We assume without loss of generality that the passband gain is 1. If $f_c > f_L$, then the filter eliminates $p_c(t)$ entirely, leaving a filtered version of $p_{s,TE}(t;x)$ as the filter output $z(t;x)$. However, unless $f_c > f_s + f_L \geqslant 2f_s$, the signal components corresponding to $S_1(f \pm f_c) = X(f \pm f_c)$ in (8) alias into the filter passband, as do the signal components corresponding to $S_n(f \pm f_c)$ for each $n > 1$. More generally, since $x(t)$ is band-limited to f_s, then $S_n(f)$, which is the $(n-1)$-fold self convolution of $S_1(f) = X(f)$, is band-limited to nf_s. Thus, the signal components corresponding to $S_n(f \pm kf_c)$ in (8) alias into the filter passband for each $k \leqslant (nf_s + f_L)/f_c$. Clearly, the distortion due to this aliasing can be made small by choosing $f_c \gg f_L$. Thus, suppose that

$$(m-1)f_s + f_L < f_c \leqslant mf_s + f_L$$

for some integer $m \geqslant 2$. Then, the spectrum of the demodulated signal $z(t;x)$, that is, the ideal low-pass filter output, can be expressed as

$$Z(f;x) = Y(f;x) + \sum_{n=m}^{\infty} \sum_{k=1}^{N(n)} \frac{(-j\pi fT)^{n-1}}{n!} [S_n(f - kf_c) + S_n(f + kf_c)] \tag{13}$$

for $|f| \leqslant f_L$, and, of course, $Z(f;x) = 0$ for $|f| > f_L$. Note that $N(n)$ in (13) is given by

$$N(n) = \left\lfloor \frac{nf_s + f_L}{f_c} \right\rfloor. \tag{14}$$

Note also that m is the smallest positive integer for which $N(m) = 1$. We remark that the sum in (13) usually contributes very little to the total distortion because $S_n(f)$ has most of its energy (or power) in the vicinity of $f = 0$ and therefore, the energy (or power) in $S_n(f \pm kf_c)$ is mostly in the vicinity of $\pm kf_c$. In other words, the signal distortion aliasing into the filter passband is very small. Thus, the distortion is dominated by the sum in (9), and we can approximate $Z(f;x)$ as

$$Z(f;x) \approx Y(f;x) = \exp(-j\pi fT)X(f) + \exp(-j\pi fT) \sum_{n=2}^{\infty} \frac{(-j\pi fT)^{n-1}}{n!} S_n(f), \quad |f| \leqslant f_L. \tag{15}$$

Furthermore, since πfT in (15) has maximum value $\pi f_L/f_c$, the coefficients $(-j\pi fT)^n/(n+1)!$ decreases rapidly with increasing n provided $f_c \gg f_L$. Hence, we can further approximate $Z(f;x)$ in the filter passband by neglecting the terms with $n > 2$ in (15) to get

$$Z(f;x) \approx \exp(-j\pi fT)X(f) - \exp(-j\pi fT) \left(\frac{j\pi fT}{2} \right) S_2(f), \quad |f| \leqslant f_L. \tag{16}$$

It follows that, ignoring the truncation, if any, of the $S_2(f)$ caused by the ideal low-pass filter, we can write the output signal $z(t;x)$ of the demodulator for a uniform-sampling TEPWM signal as

$$z(t;x) \approx x(t - T/2) - \frac{T}{2} x(t - T/2) \frac{d}{dt} x(t - T/2). \tag{17}$$

Since $h(t - T/2) \approx h(t) - (T/2)dh(t)/dt$, and $T = 1/f_c$ is usually quite small, we get that

$$\begin{aligned} z(t;x) &\approx x(t) - \frac{T}{2}(1 + x(t)) \frac{d}{dt} x(t) + \frac{T^2}{4} \left(x(t) \frac{d^2}{dt^2} x(t) + \cdots \right) \cdots \\ &\approx x(t) - \frac{T}{2}(1 + x(t)) \frac{d}{dt} x(t). \end{aligned} \tag{18}$$

In [15], we derived (18) by a different approach using a Taylor series approximation. Note that these approximations indicate that the distortion reduces in amplitude inversely with the carrier frequency f_c. In particular, the power or energy in the distortion signal should reduce at the rate of approximately 6 dB per octave as f_c increases. In Sections 2.7 and 4, we shall give numerical results in support of this conclusion.

Next, we consider natural-sampling TEPWM in which such distortion does not occur at all.

2.5. The spectra of natural-sampling TEPWM signals

In natural-sampling TEPWM, the kth pulse width τ_k is given by $\tau_k = t_k - kT$ where t_k denotes the solution to the kth crossing-point equation:

$$t_k = kT + \frac{T[1 + x(t_k)]}{2}, \quad t_k \in [kT, (k+1)T].$$

We take the viewpoint that the TEPWM signal resulting from natural sampling of $x(t)$ is the same as the TEPWM signal resulting from the uniform sampling of $\hat{x}(t)$, where $\hat{x}(t)$ is a distorted form of $x(t)$. We can then apply the uniform-sampling TEPWM results of the previous subsection to $\hat{x}(t)$ to obtain the spectrum of $\hat{p}_{\mathrm{TE}}(t;x)$, where we use the caret to distinguish this natural-sampling TEPWM signal from the uniform-sampling TEPWM signal $p_{\mathrm{TE}}(t;x)$ studied above.

In order to determine $\hat{x}(t)$, we define $\hat{t}$ as the solution to the *generalized crossing-point equation*

$$\hat{t} = t + \frac{T}{2}x(\hat{t}), \quad \hat{t} \in [t - T/2, t + T/2], \tag{19}$$

where t is any fixed real number. Note that $\hat{t} = t_k$ if we choose $t = (k + \frac{1}{2})T$. Clearly, for each choice of t, there must be at least one solution to (19), and if $\hat{t} - t - (T/2)x(\hat{t})$ is a monotone increasing function of $\hat{t}$, then the solution is unique. It is readily seen that it suffices to require that the derivative of $x(\hat{t})$ be smaller than $2/T = 2f_c$. However, we wish to have (19) define a one-one correspondence between t and $\hat{t}$, and therefore require that $x(t)$ be such that

$$\left|\frac{\mathrm{d}x(\hat{t})}{\mathrm{d}\hat{t}}\right| < \frac{2}{T} = 2f_c, \quad -\infty < \hat{t} < \infty. \tag{20}$$

Note that it is not necessary that $x(t)$ be a band-limited function just so long as (20) is satisfied. However, when $x(t)$ is a low-pass signal of bandwidth f_s, a theorem of Bernstein (cf. Theorem 6 in [18]) gives that

$$\max\left|\frac{\mathrm{d}x(t)}{\mathrm{d}t}\right| \leqslant 2\pi f_s \max|x(t)| = 2\pi f_s. \tag{21}$$

Thus, we can guarantee that (20) holds for all possible choices of low-pass functions $x(t)$ merely by requiring that $f_c > \pi f_s$. Of course, for some low-pass signals, a carrier frequency as small as the Nyquist frequency $2f_s$ will suffice to ensure that (20) is satisfied.

We hereafter assume that (20) is satisfied and hence that (19) has a unique solution for each choice of t. With $\hat{t}$ related to t via (19), we define the function $\hat{x}(t)$ as

$$\hat{x}(t) = x(\hat{t}), \quad -\infty < t < \infty \tag{22}$$

and note that the kth natural-sampling pulse width $\tau_k = T[1 + x(t_k)]/2$ for the signal $x(t)$ equals $T[1 + \hat{x}((k + \frac{1}{2})T)]/2$, that is, the kth *uniform-sampling pulse width* for the signal $\hat{x}(t + T/2)$. We note that $|\hat{x}(t)| = |x(\hat{t})| \leqslant 1$, and thus $\hat{p}_{\mathrm{TE}}(t;x)$, the TEPWM signal resulting from natural sampling of $x(t)$, is the same as $p_{\mathrm{TE}}(t;\hat{x}(t + T/2))$, the TEPWM signal resulting from uniform sampling of $\hat{x}(t + T/2)$. Therefore, we can

apply (9) to conclude that $\hat{p}_{\mathrm{TE}}(t;x)$ includes the signal

$$\hat{y}(t;x) = y(t;\hat{x}(t+T/2)) = \hat{x}(t) + \sum_{n=1}^{\infty} \frac{1}{(n+1)!} \left(\frac{-T}{2}\right)^n \frac{\mathrm{d}^n}{\mathrm{d}t^n}[\hat{x}(t)]^{n+1} \tag{23}$$

with spectrum

$$\hat{Y}(f;x) = \sum_{n=1}^{\infty} \frac{(-\mathrm{j}\pi f T)^{n-1}}{n!} \hat{S}_n(f), \tag{24}$$

where $\hat{S}_n(f)$ is the Fourier transform of $[\hat{x}(t)]^n$. More generally, the signal-dependent portion $\hat{p}_{\mathrm{s,TE}}(t;x)$ of the natural-sampling TEPWM signal has spectrum

$$\hat{P}_{\mathrm{s,TE}}(f;x) = \hat{Y}(f;x) + \sum_{k=1}^{\infty} \hat{Y}_k(f;x), \tag{25}$$

where $\hat{Y}(f;x)$ is given in (24), while for $k \geqslant 1$,

$$\hat{Y}_k(f;x) = (-1)^k \sum_{n=1}^{\infty} \frac{(-\mathrm{j}\pi f T)^{n-1}}{n!} [\hat{S}_n(f - kf_{\mathrm{c}}) + \hat{S}_n(f + kf_{\mathrm{c}})]. \tag{26}$$

Of course, (23)–(26) are unsatisfactory in that the baseband signal $\hat{y}(t;x)$ as well as the spectra $\hat{Y}_k(f;x)$ and $\hat{P}_{\mathrm{s,TE}}(f;x)$ are specified in terms of $\hat{x}(t)$ and its powers instead of $x(t)$ and its powers. We remedy this by showing that, in fact, $\hat{y}(t;x)$ as given in (23) is *precisely* $x(t)$, that is, when natural-sampling TEPWM is used, there is *no harmonic distortion* in the baseband. Nor is the demodulated signal delayed by $T/2$ with respect to the input signal (as happens in uniform-sampling TEPWM). The proof that $\hat{y}(t;x) = x(t)$ is based on the following result due to Lagrange (cf. [20, Section 7.32]).

Theorem. *Let $\phi(z)$ be analytical on and inside a contour C. Let λ be a point in C, and β be such that*

$$|\beta\phi(\alpha)| \leqslant |\alpha - \lambda|$$

for all α on the perimeter of C. Then, there is a unique $\gamma \in C$ such that

$$\gamma = \lambda + \beta\phi(\gamma)$$

and if $\psi(z)$ is any function analytical on and inside C, then

$$\psi(\gamma) = \psi(\lambda) + \sum_{n=1}^{\infty} \frac{\beta^n}{n!} \left[\frac{\mathrm{d}^{n-1}}{\mathrm{d}\theta^{n-1}} \frac{\mathrm{d}\psi(\theta)}{\mathrm{d}\theta} \phi^n(\theta)\right]\Bigg|_{\theta=\lambda}.$$

From this theorem, we get that for any integer $i > 0$,

$$\phi^i(\gamma) = \phi^i(\lambda) + \sum_{n=1}^{\infty} \frac{\beta^n}{n!} \left(\frac{i}{i+n}\right) \left[\frac{\mathrm{d}^n}{\mathrm{d}\theta^n} \phi^{n+i}(\theta)\right]\Bigg|_{\theta=\lambda} \tag{27}$$

and in particular we have that

$$\phi(\gamma) = \phi(\lambda) + \sum_{n=1}^{\infty} \frac{\beta^n}{(n+1)!} \left[\frac{\mathrm{d}^n}{\mathrm{d}\theta^n} \phi^{n+1}(\theta)\right]\Bigg|_{\theta=\lambda}. \tag{28}$$

Let C be the circle of diameter T centered at the real number t in the complex plane, and define $\phi(z) = x(\mathrm{Re}\{z\})$. Taking $\lambda = t$, we see that $\beta = T/2$ and hence from (19) and (28) we get that

$$\phi(\hat{t}) = x(\hat{t}) = \hat{x}(t) = x(t) + \sum_{n=1}^{\infty} \frac{1}{(n+1)!} \left(\frac{T}{2}\right)^n \frac{\mathrm{d}^n}{\mathrm{d}t^n}[x(t)]^{n+1}. \tag{29}$$

This result is not quite what we want, but it is nonetheless useful in its own right since it gives the signal $\hat{x}(t)$ in terms of $x(t)$ and provides a formula for *computing* the natural-sampling pulse widths from the derivatives of the powers of $x(t)$.

Given the real number t, for what number $\tilde{t}$ is t the solution to the generalized crossing-point equation? That is, we seek $\tilde{t}$ such that

$$t = \tilde{t} + \frac{T}{2}x(t).$$

Now, (22) tells us that $\hat{x}(\tilde{t}) = x(t)$, and hence we can write

$$\tilde{t} = t - \frac{T}{2}x(t) = t - \frac{T}{2}\hat{x}(\tilde{t})$$

and apply the Lagrange theorem and (28) to get that

$$\hat{x}(\tilde{t}) = x(t) = \hat{x}(t) + \sum_{n=1}^{\infty} \frac{1}{(n+1)!}\left(\frac{-T}{2}\right)^n \frac{\mathrm{d}^n}{\mathrm{d}t^n}[\hat{x}(t)]^{n+1}. \tag{30}$$

The right-hand side of (30) is the same as the right-hand side of (23) and hence, $\hat{y}(t;x) = x(t)$ which is the result that we seek. We have thus proved that when natural sampling is used, the modulating signal $x(t)$ appears *without harmonic distortion or delay* in the TEPWM modulator output. Previously, this result had been proved only for single tone and double tone signals.

More generally, from (27), we get that

$$[x(t)]^i = \sum_{m=0}^{\infty} \frac{1}{m!}\left(\frac{-T}{2}\right)^n \left(\frac{i}{i+m}\right) \frac{\mathrm{d}^m}{\mathrm{d}t^m}[\hat{x}(t)]^{m+i}. \tag{31}$$

Now, from (26) we get

$$\hat{y}_k(t;x) = (-1)^k \sum_{n=1}^{\infty} \frac{1}{n!}\left(\frac{-T}{2}\right)^{n-1} \frac{\mathrm{d}^{n-1}}{\mathrm{d}t^{n-1}}\left[2\cos(2\pi k f_c t)\cdot[\hat{x}(t)]^n\right] \tag{32}$$

and proceed to show that $\hat{y}_k(t;x)$ is also expressed quite simply in terms of $x(t)$. We express $2\cos(2\pi k f_c t)$ as $\exp(\mathrm{j}2\pi k f_c t) + \exp(-\mathrm{j}2\pi k f_c t)$, and apply the well-known result

$$\frac{\mathrm{d}^n}{\mathrm{d}t^n}(u\cdot v) = \sum_{i=0}^{n} \binom{n}{i}\left(\frac{\mathrm{d}^{n-i}u}{\mathrm{d}t^{n-i}}\right)\left(\frac{\mathrm{d}^i v}{\mathrm{d}t^i}\right)$$

to (32) to get

$$\begin{aligned}
\hat{y}_k(t;x) &= (-1)^k \sum_{n=1}^{\infty} \frac{1}{n!}\left(\frac{-T}{2}\right)^{n-1}\left[\sum_{i=0}^{n-1}\binom{n-1}{i}\left[(\mathrm{j}2\pi k f_c)^i \exp(\mathrm{j}2\pi k f_c t)\right.\right.\\
&\qquad \left.\left. +(-\mathrm{j}2\pi k f_c)^i \exp(-\mathrm{j}2\pi k f_c t)\right]\frac{\mathrm{d}^{n-i-1}}{\mathrm{d}t^{n-i-1}}[\hat{x}(t)]^n\right]\\
&= (-1)^k \sum_{i=0}^{\infty} \frac{(\mathrm{j}k\pi)^i}{i!}\left(\exp(-\mathrm{j}2\pi k f_c t)\right.\\
&\qquad \left. +(-1)^i \exp(\mathrm{j}2\pi k f_c t)\right)\sum_{m=0}^{\infty}\frac{1}{(m+i+1)m!}\left(\frac{-T}{2}\right)^m \frac{\mathrm{d}^m}{\mathrm{d}t^m}[\hat{x}(t)]^{m+i+1}\\
&= (-1)^k \sum_{i=0}^{\infty} \frac{(\mathrm{j}k\pi)^i}{(i+1)!}(\exp(-\mathrm{j}2\pi k f_c t) + (-1)^i \exp(\mathrm{j}2\pi k f_c t))[x(t)]^{i+1}
\end{aligned} \tag{33}$$

$$= \frac{(-1)^k}{\mathrm{j}k\pi}[(\exp(\mathrm{j}k\pi x(t)) - 1)\exp(-\mathrm{j}2\pi k f_c t) - (\exp(-\mathrm{j}k\pi x(t)) - 1)\exp(\mathrm{j}2\pi k f_c t)]$$

$$= \frac{2(-1)^k}{k\pi}[\sin(2\pi k f_c t) - \sin(2\pi k f_c t - k\pi x(t))], \tag{34}$$

where we used (31) to obtain (33). From (33) we get that

$$\hat{Y}_k(f;x) = (-1)^k \sum_{n=1}^{\infty} \frac{(\mathrm{j}k\pi)^{n-1}}{n!}[S_n(f + kf_c) + (-1)^{n-1} S_n(f - kf_c)] \tag{35}$$

and thus (25) becomes

$$\hat{P}_{s,\mathrm{TE}}(f;x) = X(f) + \sum_{k=1}^{\infty}(-1)^k \sum_{n=1}^{\infty} \frac{(\mathrm{j}k\pi)^{n-1}}{n!}[S_n(f + kf_c) + (-1)^{n-1} S_n(f - kf_c)]. \tag{36}$$

Note that $\hat{y}_k(t;x)$ in (34) can be viewed as having two components: the kth carrier harmonic, and the kth carrier harmonic *phase-modulated* by $x(t)$ with modulation index $k\pi$. Notice that the amplitude of the sinusoids decreases inversely while the *modulation index* increases linearly with k. In fact, since $x(t)$ satisfies (20), we see that the instantaneous frequency of $\sin(2\pi k f_c t - k\pi x(t))$ is

$$k f_c - \frac{k}{2}\frac{\mathrm{d}x}{\mathrm{d}t} > 0$$

and hence, the uniqueness of the solutions to the crossing point equations guarantees that the instantaneous frequency is always positive. Similarly, when $x(t)$ is a low-pass signal of bandwidth f_s, the instantaneous frequency is bounded below by $k(f_c - \pi f_s)$ and thus the restriction $f_c > \pi f_s$ also can be viewed as being needed to ensure that the instantaneous frequency is always positive. In any case, using (2) and (34), we can write the natural-sampling TEPWM signal $\hat{p}_{\mathrm{TE}}(t;x)$ as

$$\hat{p}_{\mathrm{TE}}(t;x) = p_c(t) + \hat{p}_{s,\mathrm{TE}}(t;x)$$

$$= x(t) + \sum_{k=1}^{\infty} \frac{2}{k\pi}\left[\sin(2\pi k f_c t) - (-1)^k \sin(2\pi k f_c t - k\pi x(t))\right]. \tag{37}$$

Note that $\hat{p}_{\mathrm{TE}}(t;x)$ consists of the modulating signal $x(t)$ together with *every* carrier harmonic and $x(t)$ phase-modulated onto each carrier harmonic, with amplitudes decreasing inversely with k.

Much to our surprise, we have not found the representation of natural-sampling TEPWM shown in (37) in the literature, even though it seems reasonable to assume that such a result must be quite well-known. After all, it is well-known that phase-modulation of a carrier by a sinusoid produces a spectrum involving Bessel functions, and, of course, so does natural-sampling TEPWM with sinusoidal input. Surely someone must already have compared the spectra and discovered that they were identical, and thus deduced that (37) holds for the special case when $x(t)$ is a sinusoid!

2.6. Demodulation of natural-sampling TEPWM signals

As with uniform-sampling TEPWM, when $x(t)$ is a low-pass signal of bandwidth f_s, an ideal low-pass filter with cut off frequency $f_L \geqslant f_s$ can be used to demodulate the natural-sampling TEPWM signal. Most of the statements made in Section 2.4 are applicable here. In particular, $\hat{Z}(f;x)$ the spectrum of the demodulated signal $\hat{z}(t;x)$, is given by

$$\hat{Z}(f;x) = X(f) + \sum_{n=m}^{\infty}\sum_{k=1}^{N(n)} \frac{(\mathrm{j}k\pi)^{n-1}}{n!}[S_n(f + kf_c) + (-1)^{n-1} S_n(f - kf_c)] \tag{38}$$

for $|f| \leqslant f_L$, and is 0 for larger values of f. Here, $N(n)$ is as defined in (14). Note that, in contrast to uniform-sampling TEPWM, there is no distortion in the baseband except for the signal components corresponding to $S_n(f \pm kf_c)$, $k > 0$ that alias into the filter passband. In fact, we can write analogously to (15) that

$$\hat{Z}(f;x) \approx X(f), \quad |f| \leqslant f_L, \tag{39}$$

which indicates that the natural-sampling TEPWM signal can be demodulated without any distortion. This is not strictly true, of course. In fact, comparing the coefficients $(\pi fT)^{n-1}$ and $(k\pi)^{n-1}$ of $S_n(f \pm kf_c)$ in (13) and (38), respectively, and noting that $fT \leqslant f_L T \ll f_c T = 1$, we see that the signal components aliasing into the filter passband are much larger in natural-sampling TEPWM than in uniform-sampling TEPWM. In the latter, these components are considerably smaller than the baseband distortion described in (9) and hence do not contribute appreciably to the total distortion. With natural-sampling TEPWM, however, these signal components are the *only* source of distortion in the baseband. As before, let m be the smallest positive integer for which $N(m) = \lfloor (mf_s + f_L)/f_c \rfloor = 1$. Then, neglecting the terms for $k > 1, n > m$ in (38), we can write

$$\hat{Z}(f;x) \approx X(f) + \frac{(j\pi)^{m-1}}{m!}[(-1)^{m-1} S_m(f - f_c) + S_m(f + f_c)], \quad |f| \leqslant f_L. \tag{40}$$

Since $\pi^{m-1}/m!$ is a decreasing function of m for $m > 3$, the distortion aliasing into the baseband can be reduced by increasing m, that is, by choosing $f_c \gg f_L, f_s$. In fact, since $m! \sim \exp(O(m \ln m))$, and $S_m(f \pm f_c)$ is small for $|f| \leqslant f_L$, the magnitude $|\hat{Z}(f) - X(f)|$ of the distortion spectrum should decrease as $\exp(-O(m \ln m))$ as m increases. Numerical results given in the next subsection seem to indicate that asymptotically the distortion actually might be decreasing as fast as $\exp(-O(m^2))$.

2.7. Example

For uniform-sampling TEPWM, the distortion signal $d(t)$ can be defined as $z(t;x) - x(t - T/2)$ where $z(t;x)$ is the inverse Fourier transform of $Z(f;x)$ as given in (13). For natural-sampling TEPWM, $d(t)$ is defined as $\hat{z}(t;x) - x(t)$ where $\hat{z}(t;x)$ is the inverse Fourier transform of $\hat{Z}(f;x)$ as given in (38). The total distortion (TD) is the energy or power of $d(t)$, and the relative total distortion (RTD) is defined as the ratio of the total distortion to the energy or power of the input signal in the filter passband, that is,

$$\mathrm{RTD} = \frac{\mathrm{TD}}{\int_{-f_L}^{f_L} \Phi_x(f)\,\mathrm{d}f}, \tag{41}$$

where $\Phi_x(f)$ is the energy or power spectral density of $x(t)$, and the integral in the denominator of (41) gives the total signal energy or power in the demodulating filter output.

We now present a numerical example to illustrate the analytical results presented above. Consider the finite energy modulating signal $x(t)=\mathrm{sinc}^2(100t)$ which has bandwidth $f_s=100$ Hz. We choose $f_L=100$ Hz also, and note that this particular input signal satisfies (20) if $f_c \geqslant 2f_s$. Thus, (33)–(40) hold for oversampling ratios as small as 2. Table 1 shows the RTD in decibels for different oversampling ratios f_c/f_s for uniform-sampling

Table 1
RTD in dB for TEPWM, $x(t) = \mathrm{sinc}^2(100t)$

f_c/f_s	2	3	4	6	8
Uniform sampling	−3.1	− 6.0	−8.5	−12.0	−14.5
Natural sampling	−16.9	−39.7	−67.0	−132.8	−207.3

and natural-sampling TEPWM. These results were obtained by numerical integration of (41). Notice that for uniform sampling TEPWM, doubling the oversampling ratio reduces RTD by about 6 dB. This supports the conclusion we drew from (17) which shows that when f_c is doubled, the energy or power of the distortion is reduced by a factor of 4. In comparison, the RTD of natural sampling TEPWM decreases much faster. In fact, for natural-sampling TEPWM, the values of the RTD in dB shown in Table 1 are well-approximated by the function $-1.525(f_c/f_s)^2 - 16.6(f_c/f_s) + 22.75$, that is, the distortion is decreasing as $\exp(-O(m^2))$.

2.8. Uniform-sampling TEPWM revisited

Next, we provide a sketch of the proof of (11), omitting many details because the argument used is similar to the one used to obtain (34). Now, the uniform-sampling pulse width $(T/2)(1 + x(kT))$ of the signal $x(t)$ can be thought of as the natural-sampling pulse width of a signal $\breve{x}(t)$ that is a distorted version of $x(t)$. Note that $\breve{x}(t)$ must be such that when it is sampled at the time instant $\breve{t}_k = t + (T/2)(1 + x(kT))$, the sample value is exactly equal to $x(kT)$. More generally, for fixed real number t, let

$$\breve{t} = t + \frac{T}{2}(1 + x(t)), \quad \breve{t} \in [t, t + T],$$

which is a monotone increasing function of t and provides a one-one map between t and $\breve{t}$ if $x(t)$ satisfies (20). Defining $\breve{x}(\breve{t}) = x(t)$ for all t, $-\infty < t < \infty$, we have the modified crossing-point equation

$$\breve{t} = t + \frac{T}{2}(1 + \breve{x}(\breve{t})).$$

Let $\breve{t}$ denote the number for which t is the solution to this crossing-point equation, that is

$$t = \breve{t} + \frac{T}{2}(1 + \breve{x}(t)).$$

It follows that $\breve{x}(t) = x(\breve{t})$, allowing us to write

$$\breve{t} = t - \frac{T}{2}(1 + \breve{x}(t)) = t - \frac{T}{2}(1 + x(\breve{t})).$$

The Lagrange theorem now gives us that

$$\begin{aligned} x(\breve{t}) = \breve{x}(t) &= \sum_{n=0}^{\infty} \frac{1}{(n+1)!} \left(\frac{-T}{2}\right)^n \frac{\mathrm{d}^n}{\mathrm{d}t^n}[x(t - t/2)]^{n+1} \\ &= x(t - T/2) + \sum_{n=2}^{\infty} \frac{1}{n!} \left(\frac{-T}{2}\right)^{n-1} \frac{\mathrm{d}^{n-1}}{\mathrm{d}t^{n-1}}[x(t - T/2)]^n \\ &= y(t; x) \end{aligned}$$

as defined in (9). We conclude that if $x(t)$ satisfies (20), then the uniform-sampling pulse widths of $x(t)$ are the same as the natural-sampling pulse widths of $y(t; x)$. It follows that (34) applies to uniform sampling of $x(t)$ and gives us $y_k(t; x)$ as defined in (11) if we replace $x(t)$ by $y(t; x)$ in the right-hand side of (34). In particular, (11) holds for all strictly lowpass signals $x(t)$ whose bandwidths f_s satisfy $\pi f_s < f_c$.

2.9. The spectra of LEPWM signals

The results for TEPWM signals obtained above are readily transformed into the corresponding results for LEPWM signals. As described briefly in Section 2.1, LEPWM signals can be thought of as being obtained by inverting the input signal $x(t)$ before applying it to a trailing-edge pulse width modulator, and then inverting the output of the modulator, that is,

$$p_{LE}(t; x) = -p_{TE}(t; -x) \quad \text{and} \quad \hat{p}_{LE}(t; x) = -\hat{p}_{TE}(t; -x).$$

Writing $p_{\mathrm{LE}}(t;x) = -p_{\mathrm{c}}(t) - p_{\mathrm{s,TE}}(t;-x) = -p_{\mathrm{c}}(t) + p_{\mathrm{s,LE}}(t;x)$, we have from (6) that

$$P_{\mathrm{s,LE}}(f;x) = \exp(-\mathrm{j}\pi fT) \sum_{k=-\infty}^{\infty} \sum_{n=1}^{\infty} \frac{(\mathrm{j}\pi fT)^{n-1}}{n!} S_n(f - kf_{\mathrm{c}}), \tag{42}$$

from which it follows that (9) and (12) give

$$p_{\mathrm{LE}}(t;x) = -y(t;-x) - \sum_{k=1}^{\infty} \frac{2}{k\pi}[\sin(2\pi kf_{\mathrm{c}}t) - (-1)^k \sin(2\pi kf_{\mathrm{c}}t - k\pi y(t;-x))] \tag{43}$$

$$= \tilde{y}(t;x) + \sum_{k=1}^{\infty} \frac{2}{k\pi}[(-1)^k \sin(2\pi kf_{\mathrm{c}}t + k\pi\tilde{y}(t;x)) - \sin(2\pi kf_{\mathrm{c}}t)], \tag{44}$$

where

$$\tilde{y}(t;x) = -y(t;-x) = x(t - T/2) + \sum_{n=2}^{\infty} \frac{1}{n!} \left(\frac{T}{2}\right)^{n-1} \frac{\mathrm{d}^{n-1}}{\mathrm{d}t^{n-1}}[x(t - T/2)]^n. \tag{45}$$

We note for future reference that in both $p_{\mathrm{s,LE}}(t;x)$ and $p_{\mathrm{s,TE}}(t;x)$, the kth pulse has width $|\tau_k - T/2| = |Tx(kT)/2|$, is positive or negative according as $x(kT)$ is positive or negative, and either begins or ends at $t = (k + \frac{1}{2})T$. In $p_{\mathrm{s,LE}}(t;x)$, positive pulses are *leading-edge* pulses that end at $t = (k + \frac{1}{2})T$, whereas in $p_{\mathrm{s,TE}}(t;x)$, positive pulses are *trailing-edge* pulses that begin at $t = (k + \frac{1}{2})T$. On the other hand, negative pulses are trailing-edge pulses in $p_{\mathrm{s,LE}}(t;x)$ and leading-edge pulses in $p_{\mathrm{s,TE}}(t;x)$.

As noted in Section 2.1, the pulse widths in a natural-sampling LEPWM signal can be different from the pulse widths in the corresponding natural-sampling TEPWM signal. The reason is that the crossing-point equations to determine the natural-sampling pulse widths are not the same in the two cases: the TEPWM modulator has pulse widths given by $t_k - kT$ where $t_k = (k + \frac{1}{2})T + Tx(t_k)/2$ whereas the LEPWM modulator has pulse widths given by $(k+1)T - t_k$ where $t_k = (k + \frac{1}{2})T - Tx(t_k)/2$. Notice, however, that in both cases, the pulse widths can be expressed as $T[1 + x(t_k)]/2$ where t_k is the solution of the appropriate crossing-point equation. From our definition that $\hat{p}_{\mathrm{LE}}(t;x) = -\hat{p}_{\mathrm{TE}}(t;-x)$ it follows that

$$\begin{aligned}\hat{p}_{\mathrm{LE}}(t;x) &= -p_{\mathrm{c}}(t) - \hat{p}_{\mathrm{s,TE}}(t;-x) \\ &= -p_{\mathrm{c}}(t) + \hat{p}_{\mathrm{s,LE}}(t;x) \\ &= x(t) + \sum_{k=1}^{\infty} \frac{2}{k\pi}[(-1)^k \sin(2\pi kf_{\mathrm{c}}t + k\pi x(t)) - \sin(2\pi kf_{\mathrm{c}}t)],\end{aligned} \tag{46}$$

where from (36) we get that the spectrum of $\hat{p}_{\mathrm{s,LE}}(t;x) = -\hat{p}_{\mathrm{s,TE}}(t;-x)$ is given by

$$\hat{P}_{\mathrm{s,LE}}(f;x) = X(f) + \sum_{k=1}^{\infty}(-1)^k \sum_{n=1}^{\infty} \frac{(\mathrm{j}k\pi)^{n-1}}{n!}[(-1)^{n-1} S_n(f + kf_{\mathrm{c}}) + S_n(f - kf_{\mathrm{c}})]. \tag{47}$$

As with uniform-sampling PWM, we have that in the natural-sampling signals $\hat{p}_{\mathrm{s,LE}}(t;x)$ and $\hat{p}_{\mathrm{s,TE}}(t;x)$, the kth pulse has width $|\tau_k - T/2| = |Tx(t_k)/2|$ (where t_k is the solution to the appropriate crossing-point equation), is positive or negative according as $x(t_k)$ is positive or negative, and either begins or ends at $t = (k + \frac{1}{2})T$. In $\hat{p}_{\mathrm{s,LE}}(t;x)$, positive pulses are *leading-edge* pulses that end at $t = (k + \frac{1}{2})T$, whereas in $\hat{p}_{\mathrm{s,TE}}(t;x)$, positive pulses are *trailing-edge* pulses that begin at $t = (k + \frac{1}{2})T$. On the other hand, negative pulses are trailing-edge pulses in $\hat{p}_{\mathrm{s,LE}}(t;x)$ and leading-edge pulses in $\hat{p}_{\mathrm{s,TE}}(t;x)$. We shall use these results in the next section to deduce the spectra of double-edge PWM signals.

3. Double-edge PWM signals with general modulation

In double-edge PWM (DEPWM) signals, the kth pulse occurs during the time interval $[kT,(k+1)T)$ which is the same as in single-edge PWM. However, it is convenient to assume that the pulse is "centered" at the midpoint $(k+\frac{1}{2})T$ of the interval rather than beginning at kT or ending at $(k+1)T$ as in TEPWM or LEPWM. DEPWM signals are either *symmetric*, in which case the kth signal sample determines the location of both edges of the kth pulse, or *asymmetric*, in which case each pulse edge location in the pulse train is determined by a different sample. Thus, in asymmetric DEPWM, the modulating signal is sampled twice during the kth pulse interval $[kT,(k+1)T)$. Nevertheless, in both these forms of DEPWM signaling, the waveform corresponding to $x(t)=0$ is $p_c(t-T/4)$, a 50% duty-cycle square wave that takes on value $+1$ for $(k+\frac{1}{4})T \leqslant t < (k+\frac{3}{4})T$ and value -1 for all other $t \in [kT,(k+1)T)$.

Uniform-sampling DEPWM signals: Both forms of DEPWM signals with uniform sampling are illustrated in Fig. 2. The carrier signal is often depicted as a sequence of ramps of alternating positive and negative slope as shown in the first graph. The second graph in Fig. 2 shows the resulting uniform-sampling symmetric DEPWM signal in which the kth pulse is positive during the time that the carrier signal is smaller than the sample value $x(kT)$. Thus, the pulse is centered exactly at $t=(k+\frac{1}{2})T$, and its width is $\tau_k = T[1+x(kT)]/2$. An alternative description (more suitable for the purposes of analysis) is that the location of the leading edge of the pulse is the time instant when a ramp with positive slope during $[kT,(k+\frac{1}{2})T)$ equals $-x(kT)$. We have shown this ramp as a dashed line in the first graph of Fig. 2. The location of the trailing edge is the time instant when the carrier ramp with positive slope during $[(k+\frac{1}{2})T,(k+1)T)$ equals $x(kT)$.

The uniform-sampling asymmetric DEPWM signal is shown in the third graph of Fig. 2. Note that the leading edges of the pulses are the same as in symmetric DEPWM, but the locations of the trailing edges are the time instants at which the carrier ramp with positive slope during $[(k+\frac{1}{2})T,(k+1)T)$ equals $x((k+\frac{1}{2})T)$, a different sample value than the one that determined the location of the leading edge. The pulse is now only *nominally* centered at $(k+\frac{1}{2})T$.

Natural-sampling DEPWM signals: Natural-sampling DEPWM signals are illustrated in Fig. 3. The first graph shows various carrier ramps and the signals $x(t)$, $-x(t)$, $\frac{1}{2}x(t)$ and $-\frac{1}{2}x(t)$. There are several different

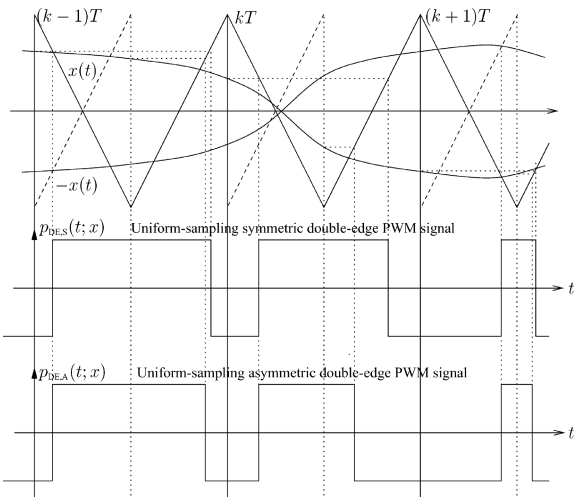

Fig. 2. Uniform-sampling double-edge PWM signals.

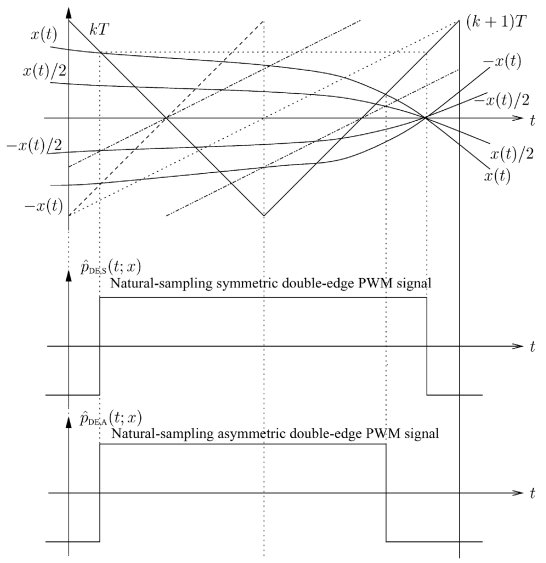

Fig. 3. Natural-sampling double-edge PWM signals.

ways that one can define the natural-sampling pulse width in *symmetric* DEPWM. Since $x(t)$ crosses the carrier twice during the pulse interval, either crossing-point could be taken as the location of one pulse edge. In the first graph of Fig. 3, we have chosen the first crossing as the location of the leading edge. Since the pulse is centered exactly at $t=(k+\frac{1}{2})T$, this also determines the location of the trailing edge, as is illustrated in Fig. 3. Alternatively, the second crossing-point could be used as the location of the trailing edge, with the leading edge being determined by symmetry, or the width given by the solution of the crossing-point equation in TEPWM could be used to determine both edge locations. Unfortunately, none of these formulations yields signals whose spectra are easy to determine. Only one of the two edge locations can be expressed as the solution of a crossing-point equation involving $x(t)$, and thus the analytical method developed in Section 2 cannot be applied without considerable extension and modification. Rather than attempt these developments, we shall simply omit natural-sampling symmetric DEPWM from further consideration in this paper.

In contrast to natural-sampling symmetric DEPWM, natural-sampling asymmetric DEPWM is much simpler to implement and to analyze. The position of the leading edge of the pulse is the time instant at which the carrier ramp with negative slope during $[kT,(k+\frac{1}{2})T)$ equals $x(t)$. As with uniform-sampling DEPWM, the location of the leading edge is also the time instant when the carrier ramp with positive slope during $[kT,(k+\frac{1}{2})T)$ equals $-x(kT)$. We have shown this ramp as a dashed line in the first graph of Fig. 3. The location of the trailing edge is the time instant when the ramp with positive slope during $[(k+\frac{1}{2})T),(k+1)T)$ equals $x(t)$. Finally, we remark that the pulse-edge locations can be thought of as being obtained by natural sampling of $-\frac{1}{2}x(t)$ and $\frac{1}{2}x(t)$ respectively by a TEPWM carrier signal that is advanced or delayed respectively by $T/4$ with respect to its usual position. This is also shown in the first graph in Fig. 3.

3.1. Uniform-sampling symmetric DEPWM signals

The kth pulse width in uniform-sampling *symmetric* DEPWM is $\tau_k=T[1+x(kT)]/2$, the same as in TEPWM or LEPWM, but the pulse is *centered* at $t=(k+\frac{1}{2})T$ instead of beginning at $t=kT$ or ending at $(k+1)T$. Thus, if $x(kT)>0$, the kth pulse can be decomposed into the sum of a positive-amplitude pulse of duration $T/2$ centered at $t=(k+\frac{1}{2})T$ and two positive-amplitude pulses: a trailing-edge pulse of duration $Tx(kT)/4$

that begins at $t=(k+\frac{3}{4})T$ and a leading-edge pulse, also of duration $Tx(kT)/4$, that ends at $t=(k+\frac{1}{4})T$. On the other hand, if $x(kT)<0$, the kth pulse can be decomposed into the sum of a positive-amplitude pulse of duration $T/2$ centered at $t=(k+\frac{1}{2})T$ and two negative-amplitude pulses: a leading-edge pulse of duration $|Tx(kT)/4|$ that ends at $t=(k+\frac{3}{4})T$ and a trailing-edge pulse of duration $|Tx(kT)/4|$ that ends at $t=(k+\frac{1}{4})T$. In other words, using our results in Section 2, we can express the uniform-sampling symmetric DEPWM signal $p_{\mathrm{DE,S}}(t;x)$ as

$$p_{\mathrm{DE,S}}(t;x)=p_{\mathrm{c}}(t-T/4)+p_{\mathrm{s,TE}}(t-T/4;x/2)+p_{\mathrm{s,LE}}(t+T/4;x/2).$$

From (6) and (42) we get that the spectrum is

$$\begin{aligned}P_{\mathrm{DE,S}}(f;x)&=\mathrm{e}^{-\mathrm{j}\pi fT/2}P_{\mathrm{c}}(f)+\mathrm{e}^{-\mathrm{j}\pi fT/2}P_{\mathrm{s,TE}}(f;x/2)+\mathrm{e}^{\mathrm{j}\pi fT/2}P_{\mathrm{s,LE}}(f;x/2)\\&=\exp(-\mathrm{j}\pi fT/2)P_{\mathrm{c}}(f)+\exp(-\mathrm{j}\pi fT)\exp(-\mathrm{j}\pi fT/2)\sum_{k=-\infty}^{\infty}\sum_{n=1}^{\infty}\frac{(-\mathrm{j}\pi fT)^{n-1}}{2^n n!}S_n(f-kf_{\mathrm{c}})\\&\quad+\exp(-\mathrm{j}\pi fT)\exp(\mathrm{j}\pi fT/2)\sum_{k=-\infty}^{\infty}\sum_{n=1}^{\infty}\frac{(\mathrm{j}\pi fT)^{n-1}}{2^n n!}S_n(f-kf_{\mathrm{c}})\qquad(48)\\&=\exp(-\mathrm{j}\pi fT/2)P_{\mathrm{c}}(f)+\exp(-\mathrm{j}\pi fT)\sum_{k=-\infty}^{\infty}\sum_{n=1}^{\infty}\frac{(\mathrm{j}\pi fT)^{2n-2}}{2^{2n-2}(2n-1)!}S_{2n-1}(f-kf_{\mathrm{c}})\cos(\pi fT/2)\\&\quad+\mathrm{j}\,\frac{(\mathrm{j}\pi fT)^{2n-1}}{2^{2n-1}(2n)!}S_{2n}(f-kf_{\mathrm{c}})\sin(\pi fT/2).\qquad(49)\end{aligned}$$

The baseband signal (corresponding to the $k=0$ terms in (48)) is

$$y_{\mathrm{DE,S}}(t;x)=\frac{1}{2}\left[x(t-3T/4)+x(t-T/4)+\sum_{n=2}^{\infty}\frac{1}{n!}\left(\frac{T}{4}\right)^{n-1}\frac{\mathrm{d}^{n-1}}{\mathrm{d}t^{n-1}}((-1)^{n-1}[x(t-3T/4)]^n+[x(t-T/4)]^n)\right].\qquad(50)$$

Proceeding as in Section 2, we use (49) to approximate the spectrum of the output of an ideal low-pass filter demodulator with cut-off frequency f_{L} as

$$Z_{\mathrm{DE,S}}(f;x)\approx\mathrm{e}^{-\mathrm{j}\pi fT}\left[X(f)\cos(\pi fT/2)-\frac{\pi fT}{4}S_2(f)\sin(\pi fT/2)\right],\qquad(51)$$

$$\approx\mathrm{e}^{-\mathrm{j}\pi fT}\left[X(f)\left[1-\frac{(\pi fT)^2}{8}\right]-\frac{(\pi fT)^2}{8}S_2(f)\right]\qquad(52)$$

for $|f|\leqslant f_{\mathrm{L}}$, where we have assumed that $f_{\mathrm{L}}\ll f_{\mathrm{c}}$ and approximated $\sin(\pi fT/2)$ and $\cos(\pi fT/2)$ by the leading terms of their Taylor series in obtaining (52) from (51). Note that there is *linear* distortion in that the input spectrum $X(f)$ is, in effect, filtered through a filter with transfer function $\cos(\pi fT/2)$. However, the effect of this filtering is small when $f_{\mathrm{L}}\ll f_{\mathrm{c}}$. Turning to the time domain, we can express the demodulator output as

$$z_{\mathrm{DE,S}}(t;x)\approx x(t-T/2)+\frac{T^2}{32}\frac{\mathrm{d}^2}{\mathrm{d}t^2}(x(t-T/2)+x^2(t-T/2)).\qquad(53)$$

Comparing this to (17), we note that the distortion term in (53) is not only considerably smaller but also decreases inversely as the square of the carrier frequency $f_{\mathrm{c}}=T^{-1}$, that is, the energy or power in the distortion reduces at roughly 12 dB per octave with increasing carrier frequency. However, it is not true, as

is sometimes believed, that the term $S_2(f)$, the primary source of second-harmonic distortion, is completely eliminated in uniform-sampling double-edge symmetric PWM.

An alternative view of a uniform-sampling symmetric DEPWM signal readily provides a slightly different (but equivalent) expression for (49) and a simple derivation of (53). Note that

$$\begin{aligned} p_{\mathrm{DE,S}}(t;x) &= p_{\mathrm{LE}}(t;[1+x]/2) + p_{\mathrm{TE}}(t;[1+x]/2) - 1 \\ &= p_{\mathrm{s,LE}}(t;[1+x]/2) + p_{\mathrm{s,TE}}(t;[1+x]/2) - 1 \end{aligned}$$

since the carrier signals $-p_{\mathrm{c}}(t)$ and $p_{\mathrm{c}}(t)$ in the LEPWM and TEPWM signals cancel out. Let $W_n(f)$ denote the Fourier transform of $[1+x(t)]^n$. Then, from (6) and (42), we get

$$\begin{aligned} P_{\mathrm{DE,S}}(f;x) &= P_{\mathrm{LE}}(f;[1+x]/2) + P_{\mathrm{TE}}(f;[1+x]/2) - \delta(f) \\ &= \mathrm{e}^{-\mathrm{j}\pi fT}\left[X(f) + 2\sum_{n=1}^{\infty} \frac{(\mathrm{j}\pi fT)^{2n}}{2^{2n+1}(2n+1)!} W_{2n+1}(f) \right. \\ &\quad \left. +2\sum_{k=1}^{\infty}\sum_{n=1}^{\infty} \frac{(\mathrm{j}\pi fT)^{2n+1}}{2^{2n+1}(2n+1)!} (W_{2n+1}(f+kf_{\mathrm{c}}) + W_{2n+1}(f-kf_{\mathrm{c}})) \right]. \end{aligned} \tag{54}$$

The baseband signal consists of the terms shown on the first line in (54) above. Taking only the term corresponding to $n=1$, we get $z_{\mathrm{DE,S}}(t;x)$ as being approximately

$$x(t-T/2) + \frac{T^2}{32}\frac{\mathrm{d}^2}{\mathrm{d}t^2}\left(x(t-T/2) + x^2(t-T/2) + \frac{1}{3}x^3(t-T/2) \right) \tag{55}$$

which is consistent with (53).

3.2. Uniform-sampling asymmetric DEPWM signals

In uniform-sampling *asymmetric* DEPWM, the kth pulse width is $\tau_k = T/2 + T[x(kT) + x((k+\frac{1}{2})T)]/4$, with a leading edge at $t = (k+\frac{1}{4})T - Tx(kT)/4$, a trailing edge at $t = (k+\frac{3}{4})T + Tx((k+\frac{1}{2})T)/4$, and a *nominal* center at $t = (k+\frac{1}{2})T$. Once again, we can decompose the pulse into the sum of a positive-amplitude pulse of duration $T/2$ centered at $t = (k+\frac{1}{2})T$ and two signal-dependent pulses that begin or end at $t = (k+\frac{1}{4})T$ and $t = (k+\frac{3}{4})T$. The signal-dependent pulses of the first type together constitute the signal $p_{\mathrm{s,LE}}(t+T/4;x/2)$ just as before. On the other hand, the signal-dependent pulses of the latter type are delayed with respect to *their* sample values $x((k+\frac{1}{2})T)$ by only $T/4$ and not by $T/2$ as in trailing-edge uniform-sampling PWM. Hence, from our results in Section 2, we get that the uniform-sampling asymmetric double-edge PWM signal $p_{\mathrm{DE,A}}(t;x)$ is

$$p_{\mathrm{DE,A}}(t;x) = p_{\mathrm{c}}(t-T/4) + p_{\mathrm{s,TE}}(t+T/4;x/2) + p_{\mathrm{s,LE}}(t+T/4;x/2),$$

while its spectrum is

$$\begin{aligned} P_{\mathrm{DE,A}}(f;x) &= \mathrm{e}^{-\mathrm{j}\pi fT/2}P_{\mathrm{c}}(f) + \mathrm{e}^{\mathrm{j}\pi fT/2}[P_{\mathrm{s,TE}}(f;x/2) + P_{\mathrm{s,LE}}(f;x/2)] \\ &= \mathrm{e}^{-\mathrm{j}\pi fT/2}P_{\mathrm{c}}(f) + \mathrm{e}^{-\mathrm{j}\pi fT/2}\sum_{k=-\infty}^{\infty}\sum_{n=1}^{\infty}\left[\frac{(-\mathrm{j}\pi fT)^{n-1}}{2^n n!} + \frac{(\mathrm{j}\pi fT)^{n-1}}{2^n n!} \right] S_n(f-kf_{\mathrm{c}}) \\ &= \mathrm{e}^{-\mathrm{j}\pi fT/2}\left[P_{\mathrm{c}}(f) + \sum_{k=-\infty}^{\infty}\sum_{n=1}^{\infty}\frac{(\mathrm{j}\pi fT)^{2n-2}}{2^{2n-2}(2n-1)!} S_{2n-1}(f-kf_{\mathrm{c}}) \right]. \end{aligned} \tag{56}$$

The baseband signal (corresponding to the $k = 0$ terms in (56)) is

$$y_{\mathrm{DE,A}}(t;x) = x(t - T/4) + \sum_{n=1}^{\infty} \frac{1}{(2n+1)!} \left(\frac{T}{4}\right)^{2n} \frac{\mathrm{d}^{2n}}{\mathrm{d}t^{2n}}[x(t - T/4)]^{2n+1} \tag{57}$$

and we can approximate the spectrum of the output of an ideal low-pass filter demodulator with cut-off frequency f_{L} as

$$Z_{\mathrm{DE,A}}(f;x) = \exp(-\mathrm{j}\pi f T/2) \left[X(f) + \frac{(\mathrm{j}2\pi f T)^2}{96} S_3(f)\right], \quad |f| \leqslant f_{\mathrm{L}}. \tag{58}$$

Notice that in contrast to (52), there is *no* linear distortion in uniform-sampling double-edge asymmetric PWM: the input spectrum appears unchanged at the output of the demodulator. Furthermore, the coefficient of the distortion is smaller in (58) than in (52). This can be explained partially by the observation that the carrier frequency has, in effect, been doubled because two samples, rather than one are being used every T seconds. However, this is not the complete story. We consider the time domain expression for the demodulator output:

$$z_{\mathrm{DE,A}}(t;x) \approx x(t - T/4) + \frac{T^2}{96} \frac{\mathrm{d}^2}{\mathrm{d}t^2}[x(t - T/4)]^3 \tag{59}$$

and note that the second-harmonic distortion noted in (53) is eliminated completely. In fact, we are left with the first and last terms exhibited on the right side of (55). From (57) it is obvious that *all* even-order harmonic distortion is absent from the output of the demodulator when uniform-sampling double-edge asymmetric PWM is used. Furthermore, since $|x^3| < x^2$ for $|x| < 1$, one can expect the second derivative in (59) to be smaller than the one in (53). However, the distortion energy or power still decreases at the rate of only 12 dB per octave as the carrier frequency increases.

3.3. Natural-sampling asymmetric DEPWM signals

Just as with uniform sampling, the kth natural-sampling asymmetric DEPWM pulse can be decomposed into the sum of a positive pulse of duration $T/2$ centered at $t=(k+\frac{1}{2})T$ and two signal-dependent pulses that begin or end at $t=(k+\frac{1}{4})T$ and $t=(k+\frac{3}{4})T$. As noted earlier. the pulse widths of these correspond to natural sampling of $-\frac{1}{2}x(t)$ and $\frac{1}{2}x(t)$ by a TEPWM signal whose carrier ramps are advanced or delayed by $T/4$ from their standard position in single-edge modulation. Alternatively, we can view these pulse widths as being obtained by standard leading-edge and trailing-edge natural sampling respectively of $\frac{1}{2}x(t - T/4)$ and $\frac{1}{2}x(t + T/4)$, and the resulting signal-dependent pulse trains are then advanced or delayed by $T/4$ respectively. In other words, the signal-dependent pulses of the first type together constitute the signal $\hat{p}_{\mathrm{s,LE}}(t + T/4; \frac{1}{2}x(t - T/4))$ while the signal-dependent pulses of the latter type together constitute the signal $\hat{p}_{\mathrm{s,TE}}(t - T/4; \frac{1}{2}x(t + T/4))$. Thus, the signal-dependent part of the natural-sampling asymmetric DEPWM signal is given by

$$\hat{p}_{\mathrm{s,DE,A}}(t;x) = \hat{p}_{\mathrm{s,LE}}(t + T/4; \tfrac{1}{2}x(t - T/4)) + \hat{p}_{\mathrm{s,TE}}(t - T/4; \tfrac{1}{2}x(t + T/4))$$

and from (36) and (47), its spectrum is

$$\begin{aligned}\hat{P}_{\mathrm{s,DE,A}}(f;x) &= \mathrm{e}^{\mathrm{j}\pi f T/2} \hat{P}_{\mathrm{s,LE}}(f; \tfrac{1}{2}x(t - T/4)) + \mathrm{e}^{-\mathrm{j}\pi f T/2} \hat{P}_{\mathrm{s,TE}}(f; \tfrac{1}{2}x(t + T/4)) \\ &= X(f) + \sum_{k=1}^{\infty} (-1)^k \sum_{n=1}^{\infty} \frac{(\mathrm{j}k\pi)^{n-1}}{2^n n!} [j^k S_n(f + kf_{\mathrm{c}}) + (-1)^{n-1}(-j)^k S_n(f - kf_{\mathrm{c}})]\end{aligned}$$

$$+\sum_{k=1}^{\infty}(-1)^k\sum_{n=1}^{\infty}\frac{(\mathrm{j}k\pi)^{n-1}}{2^n n!}[(-1)^{n-1}(-j)^k S_n(f+kf_c)+j^k S_n(f-kf_c)]$$

$$=X(f)+\sum_{k=1}^{\infty}(-1)^k\sum_{n=1}^{\infty}\frac{(\mathrm{j}k\pi)^{n-1}}{2^n n!}[S_n(f+kf_c)+S_n(f-kf_c)]\mathrm{j}^k(1+(-1)^{n+k-1}). \tag{60}$$

The quantity in parentheses in (60) has value 0 when k and n have the same parity, and value 2 when k and n have opposite parity. Hence we get that

$$\hat{P}_{\mathrm{s,DE,A}}(f;x)=X(f)+\sum_{k=1}^{\infty}(-1)^k\sum_{n=1}^{\infty}\left[\frac{(\mathrm{j}2k\pi)^{2n-2}}{2^{2n-2}(2n-1)!}(S_{2n-1}(f+2kf_c)+S_{2n-1}(f-2kf_c))\right.$$

$$\left.-\frac{(\mathrm{j}(2k-1)\pi)^{2n-1}}{\mathrm{j}2^{2n-1}(2n)!}(S_{2n}(f+(2k-1)f_c)+S_{2n}(f-(2k-1)f_c))\right]. \tag{61}$$

Comparing this to the single-edge spectrum in (36), we note that in (61), the odd carrier harmonics are being modulated by only the even powers of $x(t)$ while the even carrier harmonics are modulated by only the odd powers of $x(t)$. Furthermore, the coefficients of the various terms are smaller by factors $1/2^n$. Since the quantities in parentheses in (61) are the Fourier transforms of $2[x(t)]^{2n-1}\cos(2\pi(2k)f_c t)$ and $2[x(t)]^{2n}\cos(2\pi(2k-1)f_c t)$, we get the signal-dependent part of the natural-sampling asymmetric DEPWM signal as

$$\hat{p}_{\mathrm{s,DE,A}}(t;x)=x(t)+\sum_{k=1}^{\infty}(-1)^k\sum_{n=1}^{\infty}\left[\frac{(\mathrm{j}2k\pi)^{2n-2}}{2^{2n-2}(2n-1)!}(2[x(t)]^{2n-1}\cos(2\pi(2k)f_c t))\right.$$

$$\left.-\frac{(\mathrm{j}(2k-1)\pi)^{2n-1}}{\mathrm{j}2^{2n-1}(2n)!}(2[x(t)]^{2n}\cos(2\pi(2k-1)f_c t))\right]$$

$$=x(t)+\sum_{k=1}^{\infty}\frac{4(-1)^k}{2k\pi}\sin(2k\pi x(t)/2)\cos(2\pi(2k)f_c t)$$

$$+\sum_{k=1}^{\infty}\frac{4(-1)^k}{(2k-1)\pi}[\cos((2k-1)\pi x(t)/2)-1]\cos(2\pi(2k-1)f_c t). \tag{62}$$

But, $\sin(\theta+m\pi/2)=(-1)^k\sin(\theta)=(-1)^m(-1)^k\sin(\theta)$ if $m=2k$ is even, and $\sin(\theta+m\pi/2)=-(-1)^k\cos(\theta)=(-1)^m[(-1)^k\cos(\theta)]$ if $m=2k-1$ is odd. We apply this to (62) and combine the two sums to get

$$\hat{p}_{\mathrm{s,DE,A}}(t;x)=x(t)+\sum_{k=1}^{\infty}\frac{4(-1)^k}{k\pi}\sin(k\pi x(t)/2+k\pi/2)\cos(2\pi k f_c t)$$

$$-\sum_{k=1}^{\infty}\frac{4(-1)^k}{(2k-1)\pi}\cos(2\pi(2k-1)f_c t),$$

where the second sum can be recognized as $p_c(t-T/4)$, the DEPWM waveform when the modulator input is zero. Hence, the natural-sampling asymmetric DEPWM signal is

$$\hat{p}_{\mathrm{DE,A}}(t;x)=p_c(t-T/4)+\hat{p}_{\mathrm{s,DE,A}}(t;x)$$

$$=x(t)+\sum_{k=1}^{\infty}\frac{2(-1)^k}{k\pi}\left[\sin\left(2\pi k f_c t+k\pi\frac{x(t)+1}{2}\right)-\sin\left(2\pi k f_c t-k\pi\frac{x(t)+1}{2}\right)\right]. \tag{63}$$

As before, natural sampling produces the modulating signal without delay or distortion in the modulator output. More interestingly, (63) shows that *there are no carrier harmonics in this DEPWM signal!* All the power of the signal is in the signal-dependent terms shown in (63) and none is "wasted" in carrier harmonics.

Finally, we remark that the alternative viewpoint of treating a DEPWM signal as being obtained from the sum of a TEPWM signal and a LEPWM signal gives a very easy derivation of (63). We have that

$$\hat{p}_{\mathrm{DE,A}}(t;x) = \hat{p}_{\mathrm{TE}}(t;[1+x]/2) + \hat{p}_{\mathrm{LE}}(t;[1+x]/2) - 1$$

and substituting for $\hat{p}_{\mathrm{TE}}(t;[1+x]/2)$ and $\hat{p}_{\mathrm{LE}}(t;[1+x]/2)$ from (37) and (46) shows that the carrier harmonics cancel out to give (63) directly. However, the corresponding result for the frequency spectrum is in terms of $W_n(f)$, the Fourier transform of $[1+x(t)]^n$ as in (54), rather than in terms of $S_n(f)$, the Fourier transform of $x^n(t)$, as in (60), and is not quite as convenient.

4. Trailing-edge PWM with sinusoidal modulation

In this section, we consider modulating signals that are sinusoids or sums of sinusoids, and show that the results of the previous sections simplify into ones obtained previously by others. For simplicity, we consider only TEPWM signals. The corresponding results for LEPWM signals are easily obtained via use of the identities: $p_{\mathrm{LE}}(t;x) = -p_{\mathrm{TE}}(t;-x)$ and $J_n(-z) = (-1)^n J_n(z)$ where $J_n(\cdot)$ denotes the nth order Bessel function of the first kind, (cf.[1, Eqs. 9.1.42-43] or [6, Eqs. 8.514]). Similarly, the results for DEPWM signals can be obtained by expressing the signal-dependent portion of the DEPWM signal as the sum of the signal-dependent portions of an LEPWM signal and a TEPWM signal.

We consider natural-sampling PWM first since the results are obtained more directly.

4.1. Natural-sampling trailing-edge PWM

Let $x(t) = M\sin(2\pi f_1 t)$, with $0 \leqslant |M| \leqslant 1$, and consider the PWM signal obtained by natural sampling of $x(t)$ at frequency $f_c > \pi f_1$. From (37) we get that

$$\hat{p}_{\mathrm{TE}}(t;x) = M\sin(2\pi f_1 t) + \sum_{k=1}^{\infty} \frac{2}{k\pi}[\sin(2\pi k f_c t) - (-1)^k \sin(2\pi k f_c t - k\pi M \sin(2\pi f_1 t))].$$

We expand the term $\sin(2\pi k f_c t - k\pi M \sin(2\pi f_1 t))$ and apply the identities

$$\cos(z\sin\theta) = J_0(z) + 2\sum_{n=1}^{\infty} J_{2n}(z)\cos(2n\theta) = \sum_{n=-\infty}^{\infty} J_n(z)\cos(n\theta), \tag{64}$$

$$\sin(z\sin\theta) = 2\sum_{n=0}^{\infty} J_{2n+1}(z)\sin((2n+1)\theta) = \sum_{n=-\infty}^{\infty} J_n(z)\sin(n\theta), \tag{65}$$

where we have used the result $J_{-n}(z) = (-1)^n J_n(z)$ to simplify the summations. Collecting the terms, it is easy to show that

$$\sin(2\pi k f_c t - k\pi M\sin(2\pi f_1 t)) = \sum_{n=-\infty}^{\infty} J_n(k\pi M)\sin(2\pi(k f_c - n f_1)t). \tag{66}$$

Similarly, we have that

$$\cos(2\pi k f_c t - k\pi M\sin(2\pi f_1 t)) = \sum_{n=-\infty}^{\infty} J_n(k\pi M)\cos(2\pi(k f_c - n f_1)t). \tag{67}$$

From this we get that

$$\hat{p}_{\mathrm{TE}}(t; M\sin(2\pi f_1 t)) = M\sin(2\pi f_1 t) + \sum_{k=1}^{\infty}\frac{2}{k\pi}\left[\sin(2\pi k f_c t) - (-1)^k \sum_{n=-\infty}^{\infty} J_n(k\pi M)\sin(2\pi(kf_c - nf_1)t)\right] \tag{68}$$

$$= M\sin(2\pi f_1 t) + \sum_{k=1}^{\infty}\frac{2}{k\pi}[1-(-1)^k J_0(k\pi M)]\sin(2\pi k f_c t) - \sum_{k=1}^{\infty}(-1)^k \sum_{n=1}^{\infty}\frac{2J_n(k\pi M)}{k\pi}[\sin(2\pi(kf_c - nf_1)t) + (-1)^n \sin(2\pi(kf_c + nf_1)t)]. \tag{69}$$

The first sum in (69) consists of the carrier harmonics at frequencies kf_c. Note that the amplitude of the kth carrier harmonic is somewhat different from the $2/k\pi$ evident in (68) because the inner sum in (68) also includes a sinusoid at frequency kf_c. The double sum in (69) is the result of intermodulation between the carrier harmonics at frequencies kf_c and the signal harmonics at frequencies nf_1. When $|kf_c - nf_1| \leqslant f_L$, these intermodulation products appear at the output of the demodulating filter and give rise to distortion. Fortunately, these intermodulation products have relatively small amplitudes especially when k and n are large, and the baseband distortion at the demodulating filter output is quite small.

The spectrum of the natural-sampling PWM signal $\hat{p}_{\mathrm{TE}}(t; M\sin(2\pi f_1 t))$ is easily obtained from (69). We get that

$$\hat{P}_{\mathrm{TE}}(f; M\sin(2\pi f_1 t)) = \frac{M}{2j}[\delta(f-f_1) - \delta(f+f_1)] + \sum_{k=1}^{\infty}\frac{1-(-1)^k J_0(k\pi M)}{\mathrm{j}k\pi}[\delta(f-kf_c) - \delta(f+kf_c)] - (-1)^k \sum_{n=1}^{\infty}\frac{J_n(k\pi M)}{\mathrm{j}k\pi}[\{\delta(f-(kf_c - nf_1)) - \delta(f+(kf_c - nf_1))\} + (-1)^n\{\delta(f-(kf_c + nf_1)) - \delta(f+(kf_c + nf_1))\}], \tag{70}$$

which is exactly the result obtained by the double Fourier series method in [2,10].

The same method can be used with multiple-tone signals but the end results are more complicated. It is easy to generalize (64) and (65) by induction to get that

$$\cos\left(a + \sum_{i=1}^{m} z_i \sin\theta_i\right) = \sum_{n_1=-\infty}^{\infty}\cdots\sum_{n_m=-\infty}^{\infty}\left(\prod_{i=1}^{m} J_{n_i}(z_i)\right)\cos\left(a + \sum_{i=1}^{m} n_i\theta_i\right), \sin\left(a + \sum_{i=1}^{m} z_i \sin\theta_i\right) = \sum_{n_1=-\infty}^{\infty}\cdots\sum_{n_m=-\infty}^{\infty}\left(\prod_{i=1}^{m} J_{n_i}(z_i)\right)\sin\left(a + \sum_{i=1}^{m} n_i\theta_i\right).$$

Hence, if the m-tone modulating signal $x(t)$ is given by

$$x(t) = \sum_{i=1}^{m} M_i \sin(2\pi f_i t), \text{where } \sum_{i=1}^{m} |M_i| \leqslant 1 \tag{71}$$

and $f_c > \pi \max\{f_1, f_2, \ldots, f_m\}$, then

$$\sin\left(2\pi k f_c t - k\pi \sum_{i=1}^{m} M_i \sin(2\pi f_i t)\right) = \sum_{n_1=-\infty}^{\infty} \sum_{n_2=-\infty}^{\infty} \cdots \sum_{n_m=-\infty}^{\infty} \left(\prod_{i=1}^{m} J_{n_i}(z_i)\right) \sin\left(2\pi \left(k f_c - \sum_{i=1}^{m} n_i f_i\right) t\right)$$

which can be substituted into (37) to obtain an exact representation of the natural-sampling PWM signal with *multiple-tone* modulation. In particular, for a two-tone signal we have that the natural-sampling PWM signal is given by

$$\begin{aligned}
&\hat{p}_{\mathrm{TE}}(t; M_1 \sin(2\pi f_1 t) + M_2 \sin(2\pi f_2 t)) \\
&= M_1 \sin(2\pi f_1 t) + M_2 \sin(2\pi f_2 t) \\
&\quad + \sum_{k=1}^{\infty} \frac{2}{k\pi} \left[\sin(2\pi k f_c t) - (-1)^k \sum_{m=-\infty}^{\infty} \sum_{n=-\infty}^{\infty} J_m(k\pi M_1) J_n(k\pi M_2) \sin(2\pi (k f_c - m f_1 - n f_2) t)\right],
\end{aligned} \tag{72}$$

where we note that, owing to the contribution of the double sum in (72), the kth carrier harmonic actually has amplitude $2[1-(-1)^k J_0(k\pi M_1) J_0(k\pi M_2)]/k\pi$ and not the $2/k\pi$ evident in (72). Notice that there are tones at frequencies $k f_c \pm m f_1$ and $k f_c \pm n f_2$ arising from intermodulation of the kth carrier harmonic with the harmonics of each of the input tones. There also are tones at frequencies $k f_c \pm m f_1 \pm n f_2$ arising from intermodulation of the kth carrier harmonic with the intermodulation of the harmonics of the input tones. However, there are no intermodulation products in the baseband which contains only the modulating signal $M_1 \sin(2\pi f_1 t) + M_2 \sin(2\pi f_2 t)$. Of course, some of the tones at frequencies $k f_c \pm m f_1$, $k f_c \pm n f_2$, and $k f_c \pm m f_1 \pm n f_2$ alias into the baseband, giving some residual distortion that cannot be eliminated by the lowpass filter demodulator. The frequency spectrum is

$$\begin{aligned}
&\hat{P}_{\mathrm{TE}}(f; M_1 \sin(2\pi f_1 t) + M_2 \sin(2\pi f_2 t)) \\
&= \frac{M_1}{2j}[\delta(f - f_1) - \delta(f + f_1)] + \frac{M_2}{2j}[\delta(f - f_2) - \delta(f + f_2)] \\
&\quad + \sum_{k=1}^{\infty} \frac{1}{jk\pi}[\delta(f - k f_c) - \delta(f + k f_c)] - (-1)^k \sum_{m=-\infty}^{\infty} \sum_{n=-\infty}^{\infty} \frac{J_m(k\pi M_1) J_n(k\pi M_2)}{jk\pi} \\
&\quad \times [\delta(f - (k f_c - m f_1 - n f_2)) - \delta(f + (k f_c - m f_1 - n f_2))],
\end{aligned}$$

which is the same result as that obtained in [21] by viewing the PWM signal as a waveform composed of positive and negative staircases. The method of [21] is difficult to extend to multiple-tone inputs, and the double Fourier series method is difficult to apply even to two-tone signals. In contrast, we have outlined a new method above that easily gives exact expressions for the natural-sampling PWM signal with multiple-tone input in the time domain as well as in the frequency domain.

4.2. Uniform-sampling trailing-edge PWM

The simple technique used to obtain the spectrum of natural-sampling PWM with sinusoidal input unfortunately does not apply to uniform-sampling PWM. This is because the representation (12) of uniform-sampling PWM is in terms of $y(t)$ (as given in (9)) and not in terms of the modulating signal $x(t)$ as is the case with natural-sampling PWM. Thus, we start with (5) and proceed as follows. Let $x(t) = M\sin(2\pi f_1 t)$ where $|M| \leqslant 1$. Now, (64) and (65) are the real and imaginary parts of the Bessel identity $\exp(\mathrm{j}z\sin\theta) = \sum_{n=-\infty}^{\infty} J_n(z)\exp(\mathrm{j}n\theta)$ which can be used to write (5) as

$$\begin{aligned} P_{\mathrm{s,TE}}(f;x) &= \frac{\exp(-\mathrm{j}\pi fT)}{\mathrm{j}\pi f}\sum_{k=-\infty}^{\infty} \mathrm{e}^{-\mathrm{j}2\pi fkT}[1 - \exp(-\mathrm{j}\pi fTM\sin(2\pi f_1 kT))] \\ &= \frac{\exp(-\mathrm{j}\pi fT)}{\mathrm{j}\pi f}\sum_{k=-\infty}^{\infty}\left[\mathrm{e}^{-\mathrm{j}2\pi fkT} - \sum_{n=-\infty}^{\infty} J_n(\pi fTM)\mathrm{e}^{-\mathrm{j}2\pi(f+nf_1)kT}\right] \\ &= \frac{\exp(-\mathrm{j}\pi fT)}{\mathrm{j}\pi f}\sum_{k=-\infty}^{\infty}\left[f_{\mathrm{c}}\cdot\delta(f-kf_{\mathrm{c}}) - \sum_{n=-\infty}^{\infty} f_{\mathrm{c}}J_n(\pi fTM)\delta(f-(kf_{\mathrm{c}}-nf_1))\right], \end{aligned} \tag{73}$$

where we have used the Poisson summation formula

$$\sum_{k=-\infty}^{\infty}\mathrm{e}^{-\mathrm{j}2\pi fkT} = \frac{1}{T}\sum_{k=-\infty}^{\infty}\delta\left(f-\frac{k}{T}\right)$$

with $f_{\mathrm{c}} = 1/T$ in the last step. Note that when $k = 0$ and $n = 0$, the coefficient of $\delta(f)$ in (73) is $[\exp(-\mathrm{j}\pi fT)/(\mathrm{j}\pi f)]f_{\mathrm{c}}(1-J_0(\pi fTM))$ which can be shown to have value 0 at $f=0$ by expanding $J_0(\pi fTM)$ in a Taylor series. More generally, if $a(f)$ is continuous at f_0, then $a(f)\delta(f-f_0)=a(f_0)\delta(f-f_0)$. Applying this to $P_{\mathrm{s}}(f)$ above and adding in (3), we get

$$\begin{aligned} &P_{\mathrm{TE}}(f;M\sin(2\pi f_1 t)) \\ &= \sum_{n=1}^{\infty}(-1)^{n+1}\frac{J_n(\pi nqM)}{\mathrm{j}\pi nq}[\delta(f-nf_1)-\delta(f+nf_1)]\exp(-\mathrm{j}\pi fT) \\ &\quad + \sum_{k=1}^{\infty}\frac{[1-(-1)^k J_0(\pi kM)]}{jk\pi}[\delta(f-kf_{\mathrm{c}})-\delta(f+kf_{\mathrm{c}})] \\ &\quad - \sum_{k=1}^{\infty}\sum_{n=1}^{\infty}\exp(-\mathrm{j}\pi fT)\left[\frac{J_n(\pi(k-nq)M)}{\pi(k-nq)}(\delta(f-kf_{\mathrm{c}}+nf_1)-\delta(f+kf_{\mathrm{c}}-nf_1))\right. \\ &\quad \left. + (-1)^n\frac{J_n(\pi(k+nq)M)}{\pi(k+nq)}(\delta(f-kf_{\mathrm{c}}-nf_1)-\delta(f+kf_{\mathrm{c}}+nf_1)\right], \end{aligned} \tag{74}$$

where $q = f_1/f_{\mathrm{c}}$ is the inverse of the oversampling ratio. This result matches those obtained in [2,10] by the double Fourier series method. We restate what has often been observed before about the various terms in (74). First, the modulating sinusoid and its harmonics appear with decreasing amplitudes. We have already noted that in uniform-sampling PWM, the modulating signal and the derivatives of its powers appear in the PWM signal with a delay of $T/2$. This delay is shown explicitly in (74), but is often expressed as a factor $\exp(\mathrm{j}\pi(nq+k))$ in the usual expressions for the Fourier transform of the uniform-sampling PWM signal. We note also that the modulating tone appears with amplitude $2J_1(\pi qM)/(\pi q) \neq M$. In contrast, the modulating tone appears exactly in the natural-sampling spectrum given in (70). We conclude that uniform-sampling

PWM cannot be used to construct a *linear* amplifier but natural-sampling PWM can. However, if we assume that $f_c \gg \pi f_1$ so that $\pi q \ll 1$, then we can use the approximation $J_1(z) \approx z/2$ for small values of z (cf. [1, Eq. 9.1.7]) to assert that the input signal appears essentially without amplitude distortion in the output whenever the oversampling ratio is very large.

The analysis given above extends easily to multitone modulating signals via the generalized Bessel identity

$$\exp\left(a + \sum_{i=1}^{m} z_i \sin\theta_i\right) = \sum_{n_1=-\infty}^{\infty} \cdots \sum_{n_m=-\infty}^{\infty} \left(\prod_{i=1}^{m} J_{n_i}(z_i)\right) \exp\left(a + \sum_{i=1}^{m} n_i\theta_i\right),$$

but the results are complicated in form. If the m-tone modulating signal $x(t)$ is given by (71), then, proceeding as before, (5) becomes

$$\begin{aligned} P_s(f;x) &= \frac{\exp(-j\pi fT)}{j\pi f} \sum_{k=-\infty}^{\infty} e^{-j2\pi fkT} \left[1 - \exp\left(-j\pi fT \sum_{i=1}^{m} M_i \sin(2\pi f_i kT)\right)\right] \\ &= \frac{\exp(-j\pi fT)}{j\pi f} \sum_{k=-\infty}^{\infty} \Bigg[f_c \cdot \delta(f - kf_c) \\ &\quad - \sum_{n_1=-\infty}^{\infty} \cdots \sum_{n_m=-\infty}^{\infty} f_c \cdot \left(\prod_{i=1}^{m} J_{n_i}(\pi fTM_i)\right) \delta\left(f - kf_c + \sum_{i=1}^{m} n_i f_i\right) \Bigg] \end{aligned} \tag{75}$$

indicating the numerous intermodulation products in the baseband as well as modulated onto the carrier harmonics. In particular, we remark that the modulating tone of amplitude M_i at frequency f_i appears with amplitude

$$J_1(\pi(f_i/f_c)M_i) \prod_{\substack{l=1 \\ l\neq i}}^{m} J_0(\pi(f_l/f_c)M_l) \neq M_i$$

showing that uniform-sampling PWM distorts the relative amplitudes of the tones in the modulating signal. Such distortion does not occur with natural-sampling PWM. However, since $J_0(z) \approx 1$ for small values of z, this distortion is small if the oversampling ratio is large.

4.3. Example

When the input to a PWM modulator is a single tone or multitone signal, total harmonic distortion (THD) is most commonly used to evaluate the performance of PWM. That is, in the output signal $z(t)$ of the demodulator, *any* signal component at the same frequency as one of the tones in the modulating signal, regardless of magnitude and phase, is deemed to be the desired signal; and the distortion includes only the harmonics of the input signal tone(s) and any intermodulation products, whether present in the baseband signal $y(t)$ or aliasing into the baseband from a $y_k(t)$. This is a less stringent performance measure than the total distortion measure TD (the power in $z(t) - x(t - T/2)$ for uniform-sampling PWM and in $z(t) - x(t)$ in natural-sampling PWM) because both the amplitude distortion and phase delay of signal components in the output signal contribute to the total distortion. In this section, we use THD, which is defined as the ratio of the total power of the harmonic and intermodulation components in the baseband to the signal power in the input baseband components.

We consider the PWM signals created by uniform sampling and by natural sampling of the 4 kHz tone $x(t) = \sin 2\pi(4000)t$. The first row of Table 2 below shows the THD in dB at the output of an ideal low-pass

Table 2
THD in dB for TEPWM, $x(t) = \sin(2\pi(4000)t)$, 20 kHz ideal LPF

Oversampling ratio $1/q$	10	12	14	16	18	20
Uniform sampling	−16.0	−17.6	−19.0	−20.1	−21.2	−22.0
$20\log_{10}(\pi q/2)$	−16.1	−17.7	−19.0	−20.2	−21.2	−22.1
Natural sampling	−29.2	−53.1	−81.9	−114.5	−150.3	−189.6
$20\log_{10}((2/\pi)J_{1/q-5}(\pi))$	−29.6	−53.2	−82.0	−114.6	−150.4	−188.8

filter (LPF) of bandwidth f_L=20 kHz when uniform sampling is used. The carrier frequencies range from 40 to 80 kHz. These results were obtained by numerical computation using (69). As noted in Section 2 and exhibited in Table 1 previously, distortion in uniform-sampling PWM decreases by about 6 dB per octave with increasing carrier frequency. In fact, the distortion is almost entirely due to the second harmonic of the input tone. From (17), we get that the output of the low-pass filter includes a tone at 8 kHz of amplitude $(T/4)\cdot 2\pi(4000)=\pi q/2$ giving rise to the distortion levels shown in the second row of Table 2. As can be seen, the approximation is very close to the exact results. The third row of Table 2 shows the THD when natural sampling is used. These results were obtained by numerical computation using (74). The distortion in natural-sampling PWM is much smaller than with uniform sampling, and also decreases more rapidly with increasing carrier frequency. This distortion is almost entirely due to the signal $(2/\pi)J_n(\pi)\sin(2\pi(f_c - 4000n)t) = (2/\pi)J_n(\pi)\sin(2\pi(20000)t)$ (where $n = q^{-1} - 5$) that aliases into the very edge of the filter passband to give fifth harmonic distortion. This gives the approximate distortion shown on the fourth row of Table 2 which agrees quite well with the exact results.

Next, consider what happens when the ideal low-pass filter has bandwidth $f_L = 5$ kHz. When the oversampling ratio is an integer, there is *no* distortion in the baseband because *all* the signal harmonics are removed by the low-pass filter, as are all the carrier harmonics. Furthermore, any signal components aliasing into the baseband are at frequency $kf_c - nf_1 = 4$ kHz. Hence, there is *no* harmonic distortion whatsoever, regardless of whether natural sampling or uniform sampling is being used! Of course, complete elimination of all the signal harmonics by low-pass filtering would be difficult to achieve in practice. Also, it might be difficult in practice to maintain the oversampling ratio to be exactly an integer. Lastly, this result applies only to single tone inputs. With multi-tone inputs, intermodulation distortion *will* occur in the passband if uniform-sampling PWM is used.

Finally, we consider what happens when the input consists of tones of amplitude 0.5 at 3 and 4 kHz and $f_L = 5$ kHz. Once again, all the harmonics of the two tones are eliminated by the low-pass filter, but for uniform-sampling PWM, the two tones intermodulate to produce inband distortion at 1 kHz (and out-of-band distortion at 7 kHz,) while the second harmonic of the 3 kHz tone intermodulates with the 4 kHz tone to produce inband distortion at 2 kHz (and out-of-band distortion at 10 kHz,) and so on… to give the THD shown in the first row of Table 3. The dominant term in the distortion is the intermodulation product at

Table 3
THD for TEPWM, $x(t) = \frac{1}{2}(\sin(2\pi 4000t) + \sin(2\pi 3000t))$, 5 kHz ideal LPF

f_c	40 kHz	48 kHz	56 kHz	64 kHz	72 kHz	80 kHz
Uniform sampling	−36.9	−38.6	−40.0	−41.2	−42.2	−43.1
1 kHz intermodulation	−37.1	−38.7	−40.1	−41.2	−42.3	−43.2
Natural sampling	−111.1	−145.5	−186.6	−232.6	−282.4	−337.9
THD upper bound	−106.7	−143.3	−184.5	−229.4	−277.4	−328.0

1 kHz. From (17), we get that the approximate amplitude of this tone is $(T/8)\cdot\pi(1000)=\pi/32(f_c/4000)$ giving us that the THD is approximately $10\log_{10}([\pi/32(f_c/4000)]^2)/[2\cdot(1/2)^2])$. The values of this function are shown in the second row of Table 3. Once again, the approximation is very close to the exact results. Row 3 of Table 3 shows the THD when natural sampling is used. Since there is no intermodulation distortion present in the *baseband,* the THD is much lower than in uniform-sampling PWM. What residual distortion there is due to the aliasing of components of the form $(2/k\pi)J_m(k\pi/2)J_n(k\pi/2)\sin(2\pi(kf_c-3000m-4000n)t)$ into the baseband. A crude *upper* bound on THD can be obtained by assuming that the distortion is primarily due to the tone at frequency $f_c-3000m-4000n$ where m and n are chosen to be the smallest integers that make the frequency 5 kHz. In actuality, the net amplitude of the 5 kHz intermodulation distortion is smaller because of cancellations with other intermodulation products at 5 kHz that alias into the baseband. This bound is shown on the fourth row of Table 3 and provides a pessimistic approximation to the actual THD.

5. Concluding remarks

In this paper, we have presented a new analytical approach for the study of the frequency spectra of PWM signals. Our approach can be used with general band-limited modulating signals instead of being restricted to a single sinusoid or the sum of a few sinusoids. Exact expressions as well as approximations have been derived for the spectra of uniform-sampling and natural-sampling PWM schemes with trailing-edge and leading-edge modulation as well as with double-edge modulation, and the signals have been represented explicitly in the time domain. Our results show in great generality that there is no "harmonic distortion" of the modulating signal in the baseband for natural-sampling PWM while there is such distortion for uniform-sampling PWM, and we have characterized the distortion signals and given approximations that allow simple calculations of the distortion levels.

References

[1] M. Abramowitz, I.A. Stegun, Handbook of Mathematical Functions with Formulas, Graphs, and Mathematical Tables, US Govt. Printing Office, Washington, DC, 1968.
[2] M.M. Bech, J.K. Pedersen, F. Blaabjerg, A.M. Trzynadlowski, A methodology for true comparison of analytical and measured frequency domain spectra in random PWM converters, IEEE Trans. Power Electron. 14 (May 1999) 578–586.
[3] H.B. Black, Modulation Theory, D. Van Nostrand Co, Inc., Princeton, NJ, 1953.
[4] A. Bruce Carlson, Communication Systems, 3rd Edition, McGraw-Hill Book Company, New York, 1986.
[5] J.M. Goldberg, M.B. Sandler, New high accuracy pulse width modulation based digital-to-analogue convertor/power amplifier, IEE Proc.: Circuits Devices Systems 141 (August 1994) 315–324.
[6] I.S. Gradshteyn, I.M. Ryzhik, Table of Integrals, Series, and Products, Academic Press, Inc., New York, 1965.
[7] R.L. Kirlin, M.M. Bech, A.M. Trzynadlowski, Analysis of power and power spectral density in PWM inverters with randomized switching frequency, IEEE Trans. Ind. Electron. 49 (April 2002) 486–499.
[8] H.L. Krauss, C.W. Bostian, F.H. Raab, Solid State Radio Engineering, Wiley, New York, 1980.
[9] M. Mansuripur, The Physical Principles of Magneto-optical Recording, Cambridge University Press, Cambridge, 1995.
[10] P.H. Mellor, S.P. Leigh, B.M.G. Cheetham, Reduction of spectral distortion in class D amplifiers by an enhanced pulse width modulation sampling process, IEE Proc.-G 138 (August 1991) 441–448.
[11] D. Middleton, Introduction to Statistical Communication Theory, McGraw-Hill, New York, 1960 (reprinted by Peninsula Publishing Co., Los Altos, CA, 1987).
[12] A.V. Oppenheim, R.W. Schafer, J.R. Buck, Discrete-time Signal Processing, 2nd Edition, Prentice-Hall, Englewood Cliffs, NJ, 1999.
[13] C. Pascual, Z. Song, P.T. Krein, D.V. Sarwate, P. Midya, W.J. Roeckner, High-fidelity PWM inverter for audio amplification based on real-time DSP, IEEE Trans. Power Electron. 18 (January 2003) 473–485.
[14] G.M. Russell, Modulation and Coding in Information Systems, Prentice-Hall, Englewood Cliffs, NJ, 1962.
[15] Z. Song, D.V. Sarwate, Spectral distortion for uniform sampling pulse width modulation, in: Proceedings of the 2000 Conference on Information Sciences and Systems, Vol. II, Princeton University, New Jersey, 2000, pp. FA5.7–10.
[16] A.M. Stankovic, Random pulse modulation with applications to power electronic converters, Ph.D. Thesis, Massachusetts Institute of Technology, 1993.

[17] A.M. Stankovic, G.C. Verghese, D.J. Perrault, Analysis and synthesis of random modulation schemes for power converters, in: Proceedings of the 24th Annual IEEE Power Electronics Specialists Conference, Seattle, 1993, pp. 1068–1074.
[18] G.C. Temes, V. Barcilon, F.C. Marshall III, The optimization of bandlimited systems, Proc. IEEE 61 (February 1973) 196–234.
[19] A.M. Trzynadlowski, F. Blaabjerg, J.K. Pedersen, R.L. Kirlin, S. Legowski, Random pulse width modulation techniques for converter-fed drive systems—a review, IEEE Trans. Ind. Appl. 30 (September 1994) 1166–1175.
[20] E.T. Whittaker, G.N. Watson, A Course of Modern Analysis, 4th Edition, Cambridge University Press, Cambridge, 1952.
[21] B. Wilson, Z. Ghassemlooy, A. Lok, Spectral structure of multitone pulse width modulation, Electron. Lett. 27 (1991) 702–704.